iScience

CellPress
OPEN ACCESS

Article

Matrix Metalloprotease-7 Mediates Nucleolar Assembly and Intra-nucleolar Cleaving p53 in Gefitinib-Resistant Cancer Stem Cells

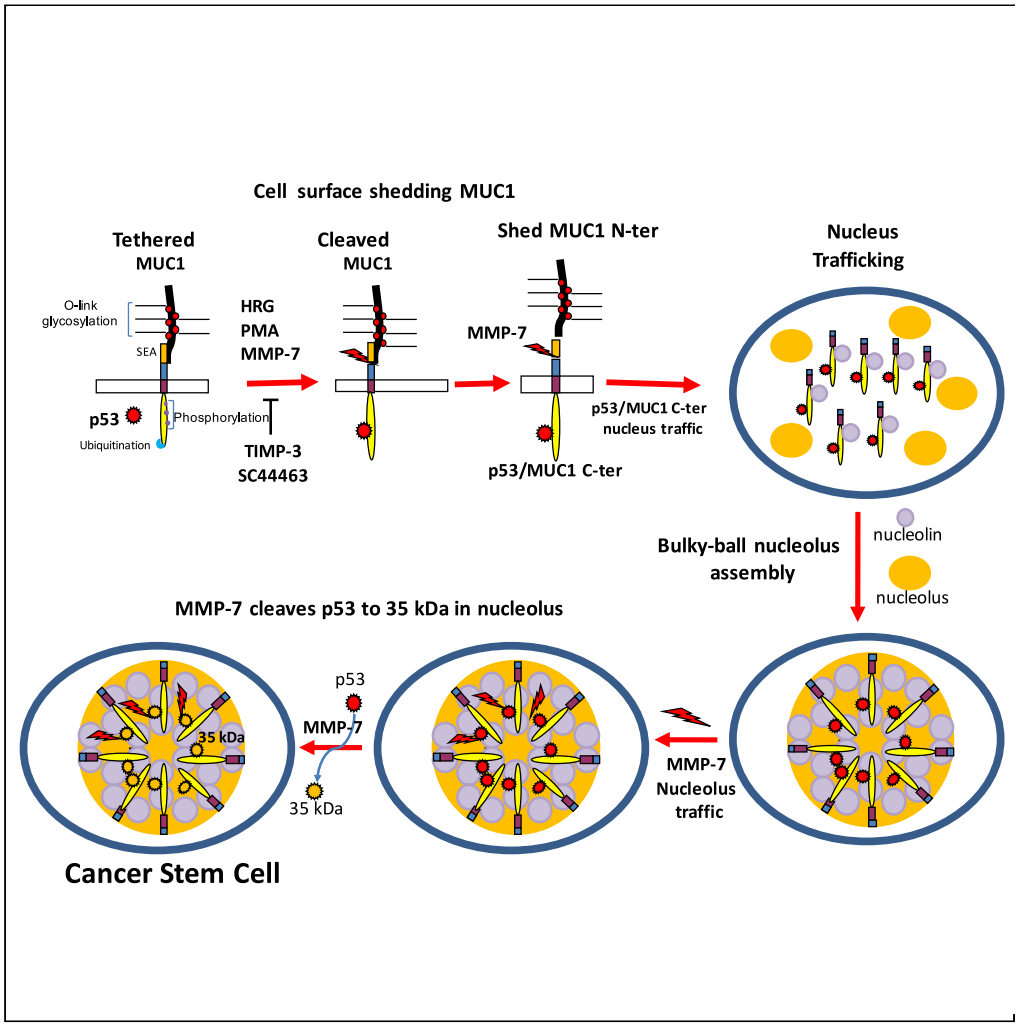

Wei-Hsuan Yu, Erxi Wu, Yongqing Li, ..., Wen-Hung Kuo, Dan Qi, Chong-Jen Yu

whyu2004@ntu.edu.tw

HIGHLIGHTS

MMP-7 cleaves the SEA domain of MUC-1 and releases MUC-1 C-ter

MUC-1 C-ter mediates bulky-ball-like nucleolus assembly trapping p53 in nucleolus

MMP-7 cleaves p53 to 35 kDa fragments in the nucleolus of gefitinib-resistant CSCs

Salinomycin induces p53 nucleoplasm translocation sensitizing CSCs to gefitinib

Yu et al., iScience *23*, 101600
October 23, 2020
https://doi.org/10.1016/j.isci.2020.101600

iScience

CellPress
OPEN ACCESS

Article

Matrix Metalloprotease-7 Mediates Nucleolar Assembly and Intra-nucleolar Cleaving p53 in Gefitinib-Resistant Cancer Stem Cells

Wei-Hsuan Yu,[1,2,10,12,*] Erxi Wu,[3,4,5,10] Yongqing Li,[6,10] Hsin-Han Hou,[7,11] Shuan-su C. Yu,[1,11] Po-Tsang Huang,[1,11] Wen-Hung Kuo,[8] Dan Qi,[3] and Chong-Jen Yu[9]

SUMMARY

The enlarged distinct bulky-ball-like nucleolus matrix assembly is observed in most cancer stem cells (CSCs); however, the underlying mechanism is largely unknown. We show that matrix metalloproteinase-7 (MMP-7) shedding MUC-1 SEA domain releases MUC-1 C-ter, facilitating the nucleolus trafficking of p53 in gefitinib-resistant lung CSCs. The nucleolus colocalizations of p53, MUC-1 C-ter, MMP-7 and nucleolin were observed in the $CD34^+$ $CXADR^+$ $CD44v_3^+$ gefitinib-resistant $EGFR^{L858R/T790M}$ CSC colonies. MUC-1 C-ter induced a unique porous bulky-ball-shaped, cagelike nucleolus that functions as a nucleus molecular "garage" for potent tumor suppressor, p53. Nucleolus could also facilitate the novel sub-nucleus compartment for proteolytic processing p53 by MMP-7 to generate a 35 kDa fragment. Moreover, we show that salinomycin, an anti-CSC agent, disrupts nucleolus by inducing nucleoplasm translocation of p53 and sensitizing CSC to chemotherapy drugs. Thus, this study highlights the MMP-7-MUC-1-p53 axis in nucleolus as a potential therapeutic target for anti-CSCs to resolve the chemotherapy-resistance dilemma.

INTRODUCTION

The nucleolus, a distinct dynamic nuclear sub-compartment, first captured the attention of cell biologists more than 100 years ago (Seshachar, 1948; Sonnenblick, 1948). Specifically, mainstream research has focused on the biological role of this mysterious dynamic sub-nuclear compartment in ribosome biogenesis and on its role as a facultative factory for protein synthesis (Carmo-Fonseca, 2015; Deisenroth and Zhang, 2010; Hernandez-Verdun and Roussel, 2003; Perrin et al., 1998; Slomnicki et al., 2016; Woods et al., 2015). The dynamic assembly and disassembly of nucleolar morphology and nucleolar functions are tightly associated with different cellular physiological or pathological states such as growth, the cell cycle, virus infection, and tumorigenesis (Orsolic et al., 2015; Takada and Kurisaki, 2015). Several cell types exhibit distinct, enlarged nucleoli such as virus-infected cells, stem cells, cancer cells, and CSCs, which has prompted studies of the biological and pathological roles of these prominent nucleolar activities (Orsolic et al., 2015; Takada and Kurisaki, 2015). Moreover, over-expression of the nucleolar proteins nucleolin and nucleostemin in sub-populations, including stem-like cancer cells, has motivated the studies of the role of nucleolar activities in CSC transformation (Bharti et al., 1996; Fonseca et al., 2015; Tin et al., 2014). Furthermore, matrix metalloproteinase-9 (MMP-9) mRNA has been shown in a single case to stabilize the activities of cytoplasmic cleaved fragments of membrane-associated nucleolin, contributing to lung cancer metastasis (Hsu et al., 2015). These findings have revealed the complexity of the facultative ribosomal protein synthesis factory, i.e., the nucleolus. In addition, the concept of a nuclear molecular cage (garage) for the temporary sequestration of potent bioactive molecules, such as oncogenic transcription factors, tumor suppressors, and stem cell factors, from their target DNAs has emerged in the past decade, and this function has been attributed to the mysterious prominent sub-nuclear compartment, the nucleolus.

Post-translational protein cleavage is thought to be responsible for the generation of cryptic bioactive molecules that promote cancer metastasis (Kryczka et al., 2012). Matrix metalloproteases (MMPs) play an important role in regulating the physiological and pathological remodeling of mammalian tissues (Behrendtsen and Werb, 1997; Cornelius et al., 1998; Lukashev and Werb, 1998; Yu et al., 2002). Of the 24 known

[1]Institute of Biochemistry and Molecular Biology, College of Medicine, National Taiwan University, Taipei 10051, Taiwan

[2]Molecular Image Center, College of Medicine. National Taiwan University, Taipei 10051, Taiwan

[3]Neuroscience Institute and Department of Neurosurgery, Baylor Scott & White Health, Temple, TX 76508, USA

[4]Colleges of Medicine and Pharmacy, Texas A&M University, Health Science Center, College Station, TX 77843, USA

[5]Livestrong Cancer Institutes and Department of Oncology, Dell Medical School, the University of Texas at Austin, Austin, TX 78712, USA

[6]Department of Surgery, University of Michigan Health Systems North Campus Research Complex, Ann Arbor, MI 48109, USA

[7]Graduate Institute of Oral Biology, College of Medicine, National Taiwan University, Taipei 10051, Taiwan

[8]Department of Surgery, National Taiwan University Hospital, Taipei 10048, Taiwan

[9]Department of Internal Medicine, National Taiwan University Hospital, Taipei 10048, Taiwan

[10]Senior authors

[11]These authors contributed equally

[12]Lead Contact

*Correspondence: whyu2004@ntu.edu.tw

https://doi.org/10.1016/j.isci.2020.101600

MMPs, most are expressed as secreted proteins that contribute to the degradation of the extracellular matrix (ECM) (Bergers et al., 2000; Bode et al., 1996; Engsig et al., 2000). MMPs can also proteolytically activate certain latent growth factors that are bound to the ECM or cell membrane (Bergers and Coussens, 2000; MacAulay et al., 2007). Moreover, cell surface docking of secreted MMPs may be necessary for their ability to degrade the ECM or activate latent growth factor receptors (Yu and Woessner, 2000). In this context, heparan sulfate proteoglycans have been proposed as docking sites for certain MMPs because MMP-7 (matrilysin) has been observed to bind to heparan sulfate glycosaminoglycans (GAGs) (Yu and Woessner, 2001). MMP-7 is a small secreted MMP that is localized on the apical surfaces of the intestinal mucosa and on endometrial and glandular epithelial cells (Woessner, 1996). Interestingly, MMP-7 is also expressed on the entire surface of carcinoma cells and mononuclear phagocytes (Woessner, 1996). Specifically, studies have shown that CD44 heparan sulfate proteoglycan (CD44HSPG; epican) recruits MMP-7 and heparin-binding epidermal growth factor precursor (pro-HB-EGF) to the surfaces of lactating mammary glands and postpartum uterine and malignant cells (Yu et al., 2002). Pro-HB-EGF is processed by MMP-7, which results in HB-EGF activating the ErbB4 receptor (Yu et al., 2002). In addition, MMP-7-induced processing of pro-HB-EGF apparently regulates the survival and remodeling of postpartum mammary and uterine tissues (Yu et al., 2002). Interestingly, MMP-7 has also been implicated in mammary and gastrointestinal tumorigenesis (Crawford et al., 2002; Matrisian et al., 1994; Rudolph-Owen et al., 1997).

The human transmembrane glycoprotein DF3/MUC-1 is aberrantly overexpressed by breast and other types of carcinomas (Kufe et al., 1984). Specifically, MUC-1 expression is localized to the apical borders of normal secretory epithelial cells. In carcinoma cells, a loss of polarity is associated with high levels of MUC-1 expression over the entire cell surface (Kufe et al., 1984). The overexpression of MUC-1 blocks apoptosis and is sufficient to confer cellular transformation (Li et al., 2003b; Yin et al., 2003). The MUC-1 protein is cleaved into N- and C-terminal subunits (N-ter and C-ter) that reside as a heterodimer at the cell membrane (Ligtenberg et al., 1992; Parry et al., 2001). The >250-kDa N-terminal ectodomain (ECD) contains variable numbers of conserved 20-amino-acid tandem repeats that are extensively modified by O-glycosylation (Gendler et al., 1988), whereas the approximately 25 kDa MUC-1 C-ter includes an extracellular region of 58 amino acids, a 28-amino-acid transmembrane domain, and a 72-amino-acid cytoplasmic tail. β-catenin, a component of the adherent junction of mammalian epithelial cells, binds directly to an SAGNGGSSL motif in the MUC-1 cytoplasmic domain (Yamamoto et al., 1997). The SAGNGGSSL motif also functions as a binding site for γ-catenin (plakoglobin) (Yamamoto et al., 1997). The MUC-1 C-ter fragment is expressed at the cell membrane and in the nucleus, where it co-localizes with β-catenin (Li et al., 2003a, 2003b) and γ-catenin (Li et al., 2003c).

The available evidence indicates that MUC-1 integrates signals from the ErbB and p53 pathways. Glycogen synthase kinase 3β (GSK3β), an effector of Wnt signaling, phosphorylates MUC-1 on a serine residue at an SPY site adjacent to that used for β-/γ-catenin binding (Li et al., 1998). Furthermore, GSK3β-mediated phosphorylation of MUC-1 decreases the interaction between MUC-1 and β-catenin (Li et al., 1998). Specifically, the tyrosine residue in the SPY site is phosphorylated by c-Src and, in contrast to the effects of GSK3β, c-Src increases the interaction between MUC-1 and β-catenin (Li et al., 2001a). Moreover, phosphorylation of the MUC-1 tail by protein kinase C (PKCδ) also contributes to the interaction between MUC-1 and β-catenin (Ren et al., 2002). Other studies have shown that MUC-1 forms a complex with epidermal growth factor receptor (EGFR) (Li et al., 2001b; Schroeder et al., 2001). The stimulation of cells with EGF is associated with tyrosine phosphorylation of the SPY site and an increase in the formation of MUC-1-β-catenin complexes (Li et al., 2001b). Conversely, the exposure of cells to heregulin (HRG), a ligand for ErbB receptors, induces the binding of MUC-1 and γ-catenin (Li et al., 2003c).

The MUC1 protein is cleaved between Gly1097 (G115 in the SEA domain) and Ser1098 (S116 in the SEA domain) within the SEA module (Parry et al., 2001; Thathiah et al., 2003). Another MUC family member, MUC-3, was found to be cleaved at a GS dipeptide sequence within the SEA module (Loukas et al., 2000), which may indicate that the conserved SEA module is cleaved by an unknown protease. Therefore, the degree of conservation in its sequence and structural features suggests that an ordered structure surrounding the cleavage site may be required for proteolysis (Wreschner et al., 2002). However, functional and structural experiments *in vitro*, *in vivo*, and even *in silico* are required to identify the MUC-1 proteolytic protease.

The enlarged distinct nucleolus observed in most stem and cancer cells reflect active ribosomal RNA assembly and protein synthesis; the novel function of the nucleolus trafficking of transcription factors could

facilitate another level regulation of protein expression. Nucleolin was documented in maintaining embryonic stem cells' self-renewal by suppressing p53 activities; however, the explicit molecular mechanism still remains to be revealed (Yang et al., 2011). How CSCs cope with rapid proliferation capacity and high protein synthesis demand is an intriguing question to be explored. Of particular interest is the molecular mechanism underlying the striking enlarged nucleolus instead of dispersed small nucleolus in the CSCs.

In this study, the facultative protease involved in proteolytic processing MUC-1 C-ter that shuttles p53 to the nucleolus is defined. Moreover, the role of the MUC-1 C-ter fragment in the formation of the distinct and enlarged nucleoli was investigated. Most importantly, the nucleolus could facilitate a novel sub-nucleus compartment for degrading p53 attributing to the anchorage-independent growth and CSC-like transformation.

RESULTS

Her-2/Neu Stimulates MMP-7-Mediated Shedding of MUC-1

MUC-1 and MMP-7 are both highly co-expressed in human breast cancer cells (Kufe et al., 1984), and active shedding of MUC-1 is associated with tumorigenesis and EMT (Li et al., 2003c). Nevertheless, the facultative physiological protease responsible for MUC-1 shedding has not yet been identified. Interestingly, HRG, PMA, and TPA can upregulate 19 kDa active MMP-7 in ZR-75-1 cells (Figure 1A). To assess whether MUC-1 is associated with active MMP-7, ZR-75-1 breast cancer cells were incubated with anti-MUC-1 N-ter and then lysed in the presence of Triton X-100. Anti-MUC-1 N-ter immunoprecipitates were analyzed by immunoblotting with anti-MMP-7. Specifically, a low level of MMP-7 was detectable in anti-MUC-1 N-ter immunoprecipitates from untreated control cells (Figure 1A). However, treatment with HRG was associated with increases in the co-immunoprecipitation (co-IP) of MUC-1 N-ter and the presence of the active 19 kDa form of MMP-7 (Figure 1A). HRG can stimulate active MMP-7 to interact with MUC-1. Similar anti-MUC-1 N-ter IP results were obtained when the cells were treated with PMA, an agent that is known to activate the shedding of diverse cell surface proteins (Hooper et al., 1997) (Figure 1A). In the reciprocal experiment, an analysis of anti-MMP-7 (RM7C) immunoprecipitates with an antibody against the MUC-1 C-ter fragment confirmed that HRG increased the physical association of MMP-7 with the MUC-1 C-ter fragment (Figure 1B). Moreover, the expression of MUC-1 C-ter as multiple fragments suggests that it is subject to proteolytic cleavage (Figure 1B). Similar anti-MMP-7 IP results were obtained in PMA-treated ZR-75-1 cells (Figure 1B). To assess the contribution of MMP-7 to the cleavage of the MUC-1 C-ter fragment, ZR-75-1 cells were transfected to express an empty vector or MMP-7. An immunoblot analysis of anti-MMP-7 immunoprecipitates with anti-MUC-1 C-ter demonstrated that the interaction with MMP-7 was associated with MUC-1 C-ter cleavage (Figure 1C). These findings indicate that the interaction between MMP-7 and MUC-1 is stimulated by HRG and PMA and is associated with the cleavage of MUC-1 C-ter fragments.

MMP-7 Cleaves the MUC-1 SEA Domain

To further assess the effects of MMP-7, anti-MUC-1 N-ter immunoprecipitates were prepared from ZR-75-1 cells. An immunoblot analysis of the precipitates with anti-MUC-1 C-ter demonstrated that the MUC-1 C-ter fragment co-precipitated with the N-ter fragment (Figure 1D, lane 1). However, treatment of the anti-MUC-1 N-ter immunoprecipitates with MMP-7 led to the release of multiple MUC-1 C-ter fragments from the complex, suggesting the presence of multiple cleavage sites for MMP-7 (Figure 1D, lane 2). As a control, an MMP-7 inhibitor, SC44463, was added to the cells, which blocked MMP-7-mediated cleavage of the MUC-1 complex (Figure 1D, lane 3). To identify the cleavage site, a 102-amino-acid MUC-1 extracellular domain (ECD) was fused to a human Fc fragment. Incubation of the MUC-1 (ECD)-Fc fusion protein with recombinant MMP-7 was associated with cleavage that generated an approximately 20-kDa-fragment (Figure 1E). The N-terminal amino acid sequencing of the fragment demonstrated a novel cleavage site between Pro1145 and Phe1146. In contrast, the MUC-1 (ECD)-Fc fusion protein did not appear to be cleaved when SC44463 and MMP-7 were added to the cells (Figure 1E). Moreover, the MUC-1 (ECD)-Fc fusion protein was not cleaved by recombinant active MMP-2 or MMP-9 (Figure 1E). These findings indicate that MMP-7 acts as a MUC-1 sheddase by cleaving the MUC-1 ECD at the "PF" site. From the *in vitro* digestion by purified recombinant active MMP-7 digestion results, MMP-7 can cleave MUC-1 in the multiple fragments between 21 kDa and 16 kDa (Figure 1C). There are three putative cleavage sites in the SEA domain region. The first putative cleavage site in the SEA domain of MUC-1 is KFRPG↓SVVV, which is further validated by a hypothetical docking model (Figure 2). Two other putative cleavage sites are reported as MMP-7 consensus cleavage sites, VVQ↓ LTL and RYN↓LTIS (Lin et al., 2001; Eckhard et al., 2016). The novel

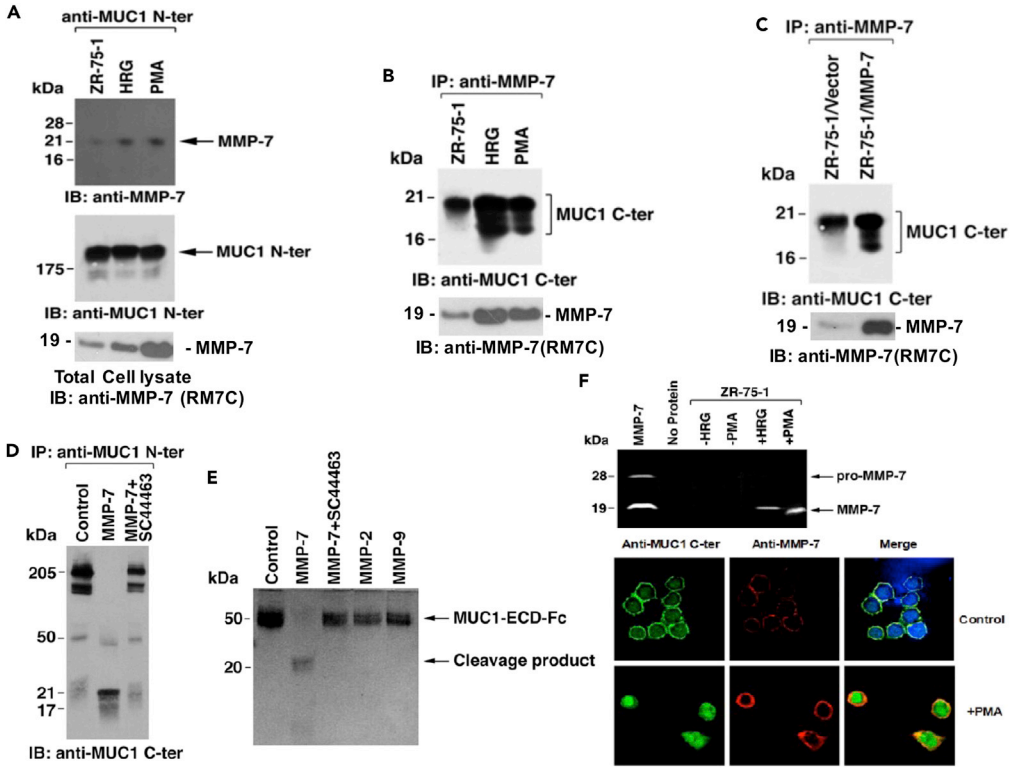

Figure 1. HRG and PMA Induce MUC-1 Shedding by MMP-7

(A) ZR-75-1 cells were treated with HRG or PMA for 30 min and subjected to immunoprecipitation with anti-MUC-1 N-ter Ab. The precipitates were analyzed by immunoblotting with anti-MMP-7 (RM7C) polyclonal Ab and anti-MUC-1 N-ter. Bottom panel: the total cell lysates were also immunoblotted with anti-MMP-7 (RM7C) polyclonal Ab.

(B) Anti-MMP-7 immunoprecipitates from HRG- or PMA-treated cells were analyzed by immunoblotting with anti-MUC-1 C-ter.

(C) ZR-75-1 cells were transfected to express an empty vector or MMP-7 and selected for 5 days in the presence of blasticidin-S. Anti-MMP-7 immunoprecipitates were analyzed by immunoblotting with anti-MUC-1 C-ter.

(D) MMP-7 functions as an MUC-1 sheddase by cleaving MUC 1-ECD-Fc. Anti-MUC-1 N-ter immune precipitates from ZR-75-1 cells were incubated with MMP-7 alone and in the presence of SC44463. The proteins were subjected to an immunoblot analysis (non-denaturing conditions) with anti-MUC-1 C-ter.

(E) An MUC-1 extracellular domain (ECD)-Fc fusion protein was incubated with 20 ng MMP-7 (alone and in the presence of SC44463), 40 ng MMP-2, or 40 ng MMP-9. The products were analyzed by SDS-PAGE and Coomassie Blue staining (upper panel). The N-terminal amino acid sequencing of the approximately 20-kDa band (lane 2) revealed cleavage at the PF site (lower panel).

(F) Upper panel: lysates from untreated, HRG- and PMA-treated ZR-75-1 cells were subjected to immunoprecipitation with anti-MMP-7. MMP-7 activity was assessed by CM-transferin zymography. Pro-MMP-7 and MMP-7 were included as controls (lane 1). Lower panel: MCF-10A cells were stimulated with PMA, fixed, and stained with anti-MUC-1 C-ter and anti-MMP-7.

cleavage site defined by the N-terminal amino acid sequencing of the fragment from the MUC-1(ECD)-Fc fusion proteins demonstrated a novel cleavage site between Pro1145 and Phe1146 (Figure 1E).

Cleavage of the MUC-1 SEA Domain by Mature MMP-7 Induces Conformational Changes in the SEA Domain

As the *in vitro* results indicated that MMP-7 might interact with MUC-1 C-ter, we then examined the working hypothesis *in silico* and in a more precise manner using the MUC-1 SEA domain and mature MMP-7. The docking results showed that the Gly-loop (K111FRPG↓SVVV119) (Pelaseyed et al., 2013) of the MUC-1 SEA domain (based on PDB code: 2ACM)/MMP-7 (based on PDB code: 2Y6D) complexes may snake into the mature MMP-7 active site with E121 and His (H120, H124, H130) coordinated zinc and water upon cleavage of the MUC-1 SEA domain (Figure 2A). The proteolytic cleavage was also investigated using *in vitro*

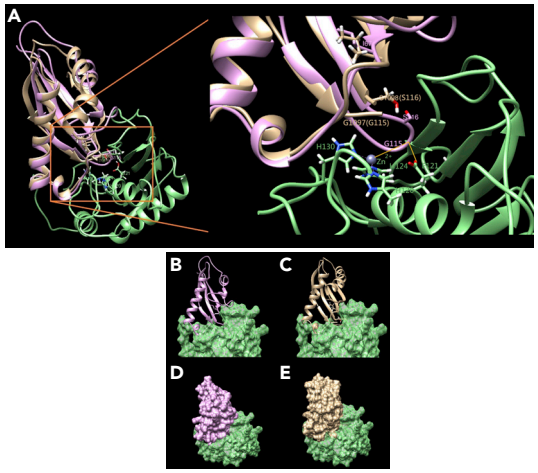

F KFRNPG↓SVVVQ↓LTLAFREGTINVHDVETQFNQYKTEAASRYN↓LTISDVP↓FP↓FSAQSGAG

Figure 2. MUC-1 SEA Domain Complexes with Active MMP-7 *in Silico*docking Model

(A) Comparison of the docking models for the MUC-1 SEA domain/mature MMP-7 complexes upon cleavage of the MUC-1 SEA domain (based on PDB code: 2ACM). The enlarged window shows a clearer image of the loop near the cleavage site (G1097-S1098 (SEA domain: G115-S116)) snaking into the active site of mature MMP-7 (based on PDB code: 2Y6D; H120, H124, H130 E121 (pro-MMP-7: H219, H223, H229, E220)). The cleaved and uncleaved MUC-1 SEA domain molecules are indicated by tan and orchid ribbons. The mature MMP-7 molecule is presented as a spring green ribbon.

(B and C) The binding complexes are shown as a spring green surface in mature MMP-7 and cleaved (C) and uncleaved (B) MUC-1 SEA domain molecules as tan and orchid ribbons. The two loops of the MUC-1 SEA domain shrink after G1097-S1098 site cleavage.

(D and E) The binding complexes are presented as a spring green surface in mature MMP-7 and cleaved (E) and uncleaved (D) MUC-1 SEA domain molecules as tan and orchid surfaces. (E) The contact area between the MUC-1 SEA domain and mature MMP-7 decreases after cleavage.

(F) Blue arrows indicate the putative MMP-7 specific cleavage sites in the SEA domain sequence. Red arrows indicate the N-terminal sequencing for the MMP-7 cleaves MUC-1 (ECD)-Fc fusion proteins products.

cleavage experiments. The Gly-Ser-loop was bound and cleaved by MMP-7 (Figure 1) and then the loop was removed from the active site of MMP-7 to form part of the β-3 sheet of MUC-1 (Figures 2B and 2C). In addition, the interaction surface between the MUC-1 SEA domain and MMP-7 seemed to change due to the conformational changes in the un-cleaved/cleaved MUC-1 SEA domains. According to the contact surface calculation for the MUC-1 C-ter/MMP-7 complex upon cleavage of MUC-1 C-ter, the contact area decreased after the G1097-S1098 site of the loop was cleaved from 3645 $Å^2$ to 3164 $Å^2$ (Figures 2D and 2E). These findings highlight the need to validate this hypothetical model by studying the colocalization of MUC-1 and mature MMP-7 by immunofluorescence with double staining and assessing purified *E. coli*-derived recombinant MMP-7 proteolysis at the cell culture level.

To confirm the involvement of MMP-7 in the shedding of MUC-1 in cell culture, ZR-75-1 cells were incubated with purified *E. coli*-derived recombinant active MMP-7 and then analyzed for cell surface anti-MUC-1 N-ter reactivity by confocal microscopy. The results demonstrated that treatment with recombinant active MMP-7 decreased the cell surface reactivity of anti-MUC-1 N-ter (Figure 3A). As a control, the effect of MMP-7 on MUC-1 shedding was efficiently blocked by TIMP-3 but not TIMP-1 or TIMP-2 (Figure 3A). As an additional control, the cells were incubated with recombinant MMP-9, which had no detectable effect on the release of the MUC-1 N-ter fragment (Figure 3A).

HRG and PMA Induce Nucleolus Localization of the MUC-1 C-Ter through Upregulating MMP-7 Expression while Inhibited by TIMP-3

Little is known about the fate of the C-ter fragment after shedding of the MUC-1 ectodomain. However, the studies have demonstrated that HRG induces the localization of the MUC-1 C-ter fragment and γ-catenin to the nucleolus (Li et al., 2003c). To assess whether MMP-7 mediates the nucleolar localization of the MUC-1 C-ter fragment, MCF-10A and ZR-75 cells were stained with anti-MUC-1 C-ter and analyzed by confocal

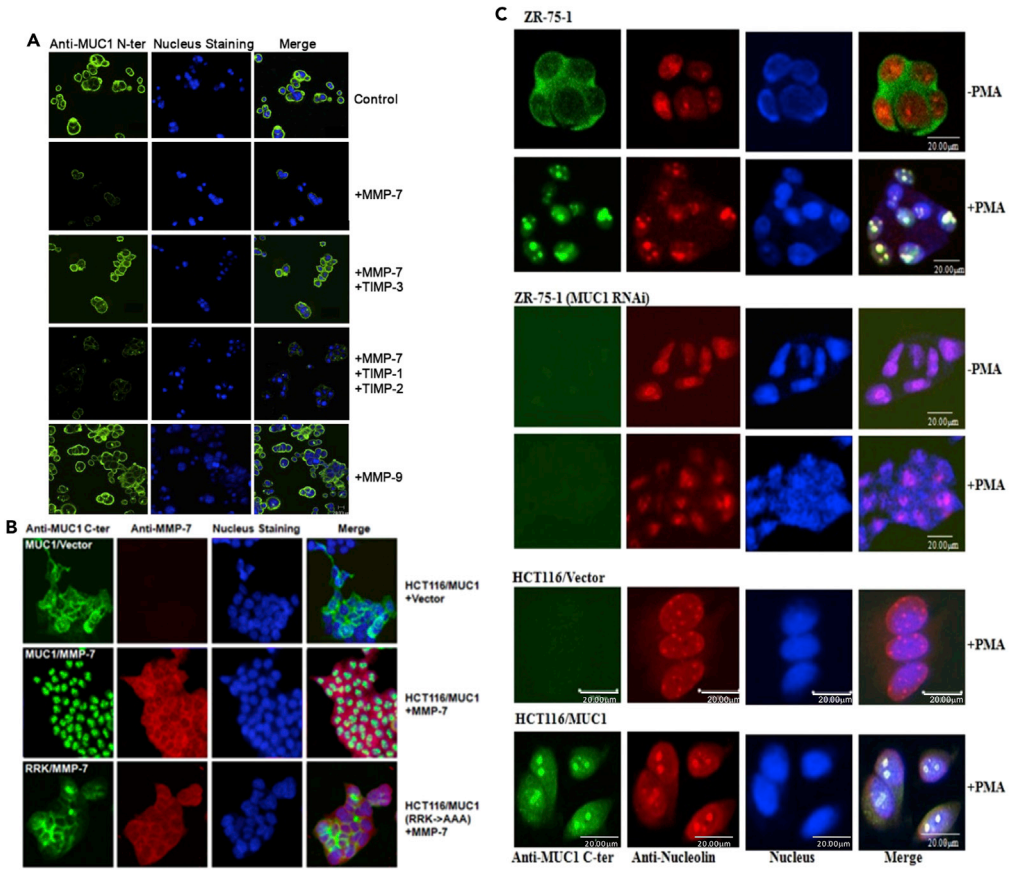

Figure 3. MMP-7 Shedding MUC-1 Releases MUC-1 C-Ter Inducing Nucleolus Translocation and Distinct Enlarged Nucleolus

(A) ZR-75-1 cells were treated with the indicated recombinant proteins for 4 h. The cells were then fixed and stained with anti-MUC-1 N-ter. The nuclei were stained with TOTO-3.

(B) HCT116/MUC-1 and HCT116/MUC-1(RRK→AAA) cells were transfected to express the empty vector or MMP-7 and selected in blasticidin-S for 5 days. The cells were fixed and stained with anti-MUC-1 C-ter and anti-MMP-7. The nuclei were stained with TOTO-3.

(C) MUC-1 C-ter induces distinct, enlarged nucleoli. ZR-75-1 cells were infected with a retrovirus expressing the empty vector or MUC-1 siRNA and grown for the indicated number of days. Lysates from the cells were analyzed by immunoblotting with anti-MUC-1 N-ter and anti-tubulin. ZR-75-1 cells expressing the empty retroviral vector (top two panels) of MUC-1 siRNA (middle two panels) were left untreated or exposed to PMA for 60 min. HCH116 cells were stained with anti-MUC-1 C-ter, anti-nucleolin, and TOTO-3. Bottom panels: HCT116/vector and HCT116/MUC-1 cells were treated with PMA and stained with anti-MUC-1 C-ter, anti-nucleolin, and TOTO-3.

microscopy. The MUC-1 C-ter fragment was detectable at the cell membrane of the control MCF10A and ZR-75 cells (Figures 1F lower panel and 3A). As previously demonstrated (Kufe et al., 1984), after stimulation with HRG or PMA, the MUC-1 C-ter fragment localized to discrete bodies within the nucleus (Figures 1F lower panel and 3C). Importantly, TIMP-3, but not TIMP-1/-2, inhibited HRG-induced nuclear targeting of MUC-1, which suggests that this event is mediated by MMP-7 (Figure 3A). To validate that these concentric intra-nuclear compartments were the nucleolus, a monoclonal antibody against a nucleolus-resident protein, nucleolin, was used to co-stain cells immune-fluorescently with anti-MMP-7 (RM7C). The treatment of cells with PMA or recombinant MMP-7 directly resulted in a similar pattern of nuclear MUC-1 C-ter and nucleolin colocalization (Figures 3B and 3C). Because these results indicated that HRG could activate MMP-7, we measured MMP-7 activity in control and HRG-treated cells by CM-transferrin zymography. The zymograms demonstrated that HRG markedly increased active MMP-7 activity compared with the control cells (Figure 1F upper panel). Similar results were obtained following PMA stimulation (Figure 1F upper panel). To determine whether the response was obtained in other cells, the nontransformed human breast epithelial cell line MCF-10A was subjected to confocal microscopy (Soule et al., 1990). MCF-10A cells expressed

MUC-1 C-ter predominantly at the cell membrane (Figure 1F lower panel), and similar findings were obtained for MMP-7 expression (Figure 1F). PMA treatment of MCF-10A cells was associated with the localization of the MUC-1 C-ter fragment to the nucleus (Figure 1F lower panel). As found in ZR-75-1 cells, PMA treatment also resulted in the nuclear targeting of MUC-1 C-ter (Figure 3C). These findings indicate that HRG and PMA target MUC-1 C-ter the nucleus via an MMP-7-mediated mechanism.

MUC-1 Is Required for MMP-7-Induced Nucleolar Assembly

To further investigate the role of MMP-7 in the modulation of MUC-1 signaling, human HCT116 carcinoma cells, which do not express detectable levels of MUC-1, were analyzed by immunoblotting and RT-PCR. HCT116 cells stably transfected with MUC-1 (Ren et al., 2002) expressed the C-ter fragment at the cell membrane (Figure 3B). By contrast, MMP-7 expression was associated with the redistribution of MUC-1 C-ter in the nucleus (Figure 3B). MUC-1 C-ter contains an RRK motif that may function in nuclear localization. Consequently, we mutated RRK→AAA in full-length MUC-1 and stably expressed this mutant in HCT116 cells (Li et al., 2003c). Similar to wild-type MUC-1, MUC-1(RRK→AAA) C-ter was expressed at the cell membrane (Li et al., 2003c). The redistribution of the MUC-1(RRK→AAA) mutant was associated with MMP-7 expression, but unlike wild-type (Li et al., 2003c), the MUC-1(RRK→AAA) C-ter fragment localized to the perinuclear region (Figure 3B). To determine whether the localization of MUC-1 C-ter to the nucleolus could affect the nucleolar structure, the expression of MUC-1 was knocked-down in ZR-75-1 cells by infection with a retrovirus expressing small interfering RNA (siRNAP duplexes that target MUC-1). In contrast to transfection with a virus expressing the empty vector, infection with the MUC-1 siRNA virus was associated with the downregulation of MUC-1 on days 5 and 10. The treatment of ZR-75-1/vector cells with PMA was associated with the formation of distinct, enlarged nucleoli compared with the nucleoli in untreated cells (Figure 3C upper panel). By contrast, PMA treatment had little, if any, effect on the nucleolar structure in ZR-75-1/MUC-1 siRNA cells (Figure 3C middle panel). Moreover, PMA treatment of $HCT116^{MUC-1}$ cells, but not $HCT116^{vector}$ cells, was associated with the formation of discrete enlarged nucleoli (Figure 3C lower panel).

Disruption of MMP-7-MUC-1 Signaling Alters the Anchorage-Independent Growth of ZR-75-1 Cells

ZR-75-1 cells grow on plastic as foci of multilayered aggregates or domes (Figure 4A upper panel). Treatment with the MMP-7 inhibitor SC44463 was associated with an altered growth pattern in which the foci consisted of only a single layer of cells (Figure 4A middle panel). TIMP-3 also abrogated the formation of ZR-75-1 cell domes (Figure 4A middle panel). In concert with these findings and in contrast to wild-type MMP-7, the incubation of cells with a dominant-negative MMP-7 (E219Q) (Yu et al., 2002) resulted in growth as flat foci (Figure 4A lower panel). Moreover, ZR-75-1 cells infected with the empty retroviral vector grew as multilayered domes (Figure 4C). Conversely, knocking down MUC-1 expression (Figure 4B) was associated with growth as flat foci similar to the effect obtained upon the inhibition of MMP-7 (Figure 4C). Notably, cells with distinct, enlarged nucleoli were observed in the upper layers of cells and not those attached to the substrate. These findings indicate that the anchorage-independent growth of ZR-75-1 cells is altered by the disruption of MMP-7-MUC-1 signaling.

MMP-7-MUC-1 Signaling Disrupts the Formation of Mammary Acinar Structures

MCF-10A cells grown in Matrigel form acinar structures (Petersen, 1992; Weaver, 1997), and an analysis of MCF-10A cell acini demonstrated the localization of MUC-1 C-ter at the cell surface (Figure 4D upper panel). Moreover, the apical expression of MUC-1 C-ter was more prominent than that detected at the basolateral surfaces, reflecting the positioning of MUC-1 in normal mammary epithelium (Figure 4D upper panel). Treatment with PMA was associated with the formation of complex multiacinar structures and the filling of the lumens (Figure 4D left middle panel). As observed for cells grown on plastic, PMA also induced the localization of MUC-1 C-ter in discrete nuclear structures (Figure 4D left middle panel). Furthermore, recombinant TIMP-3 inhibited both the PMA-induced disruption of acinar structure and the nuclear targeting of MUC-1 C-ter complexes, which indicated that these responses were induced by MMP-7 (Figure 4D lower panel). To directly assess the effects of MMP-7, MCF-10A cells in Matrigel were treated with recombinant MMP-7. The resultant images showed that, similar to PMA, MMP-7 induced complex multiacinar structures with the filling of the lumens and targeted MUC-1 C-ter to the nucleus (Figure 4D right middle panel). As a control, the cells were treated with SC44463, which blocked the MMP-7-induced disruption of the acinar structure and nucleolar targeting of MUC-1 C-ter (Figure 4D right lower panel). The enlarged concentric nucleolus was found in MMP-7pEF6V5 vector-transfected MUC-1-positive ZR-75-1 cells. The results implicate that both MMP-7 and MUC-1 are required for the enlarged nucleolus formation in breast carcinoma tissue (Figure 4). MMP-7 is overexpressed in certain human invasive

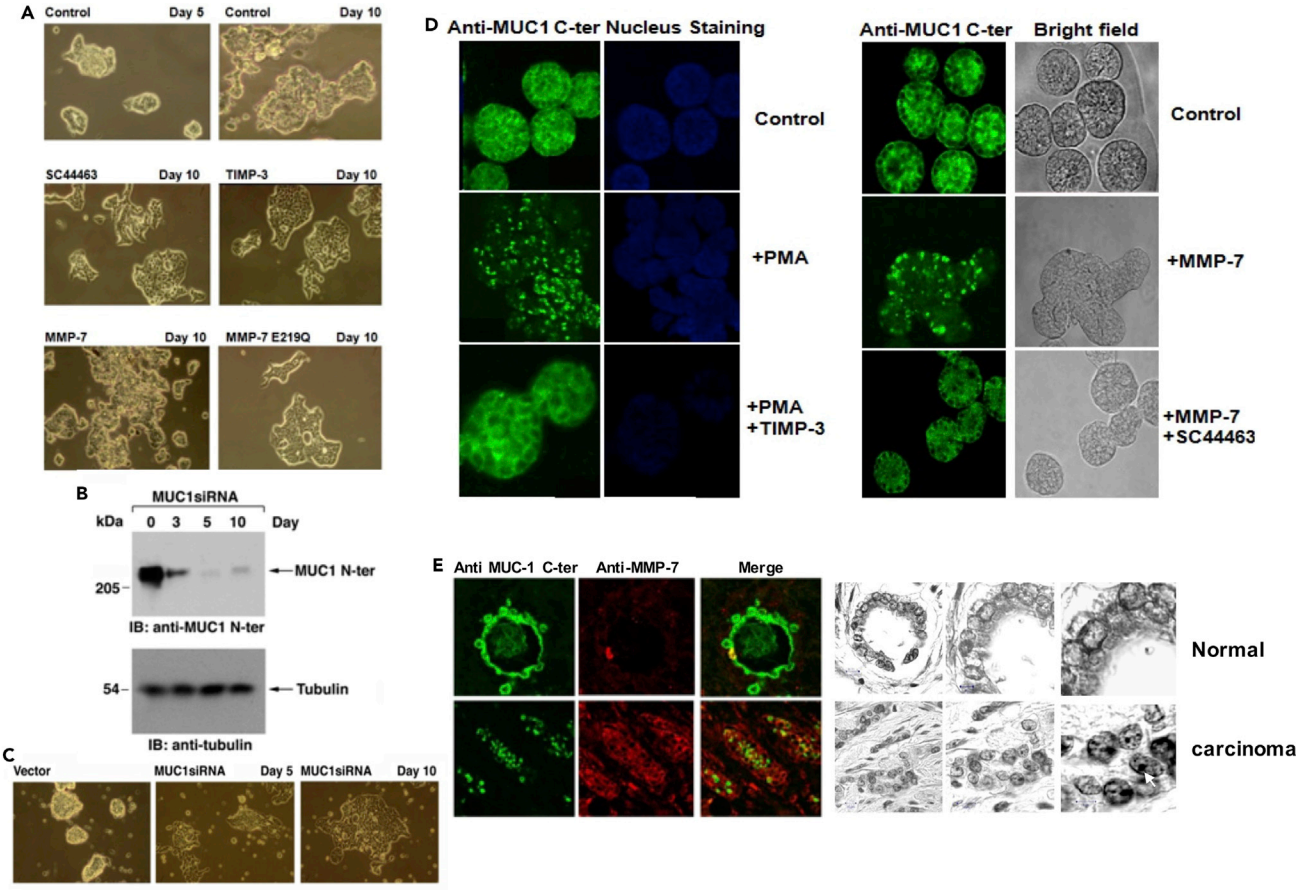

Figure 4. Co-expression of MUC-1 and MMP-7 Confirms the Anchorage Independent Growth Phenotypes

(A) Top panel: ZR-75-1 cells grown in flasks for 5 and 10 days exhibited foci of multilayered domes. Middle panel: cells grown for 10 days in the presence of SC44463 or TIMP-3 exhibited flat foci consisting of a single layer of cells. Lower Panel: the cells were grown for 10 days in the presence of MMP-7 or the dominant-negative MMP-7 E219Q.

(B) Lysates from the cells were analyzed by immunoblotting with anti-MUC-1 N-ter and anti-α-tubulin (lower panels).

(C) The cells were infected with a retrovirus expressing the empty vector or MUC-1 siRNA and grown for 5 or 10 days.

(D) MMP-7 → MUC-1 signaling induces the formation of complex multi-acinar structures and targets MUC-1 C-ter to the nucleolus in MCF-10A 3D culture assay: (Top panels) MCF-10A cells were cultured for 10 days in Matrigel containing PMA or MMP-7 in the absence and presence of TIMP-3 or SC44463. The cells were fixed and stained with anti-MUC-1 C-ter. The nuclei were stained with TOTO-3. (Middle panels) MCF-10A cells were cultured for 10 days in Matrigel containing PMA in the absence and presence of TIMP-3. The cells were fixed and stained with anti-MUC-1 C-ter. The nuclei were stained with TOTO-3. (Bottom panels) MCF-10A cells were cultured for 10 days in Matrigel containing MMP-7 in the absence or presence of SC44463.

(E) Left panel: sections of normal mammary ductal epithelium and an invasive ductal carcinoma were assessed to visualize their reactivity with anti-MUC-1 C-ter and anti-MMP-7. Right panel: enlarged concentric nucleoli were observed in breast carcinoma cells but not normal mammary gland epithelial cells.

breast carcinomas (Pacheco et al., 1998). To assess the distribution of MMP-7 and MUC-1 in human mammary tissues, studies were first performed to assess normal ductal epithelium, but MMP-7 expression was minimally detectable in the cells lining the ducts, and the expression of MUC-1 C-ter was localized to the apical cell membrane (Figure 4E left upper panel). Conversely, in invasive breast carcinoma, MMP-7 expression was readily detectable and localized over the entire cell surface (Figure 4E left lower panel). The pattern of MUC-1 C-ter expression in invasive carcinoma was consistent with a loss of polarity (Figure 4E left lower panel). In addition, the colocalization of MMP-7 and MUC-1 C-ter was not apparent (Figure 4E left lower panel). Moreover, the nucleolus distribution of MUC-1 C-ter in invasive breast carcinoma showed the correlation of the expression of MMP-7 with the polarity alteration and revealed the clear, distinct, and enlarged nucleoli (Figure 4E).

The Nucleolar Translocation of p53 Is MMP-7/MUC-1 C-Ter Dependent in Colon Cancer

Interestingly, MMP-7-mediated proteolytic processing of MUC-1 and the release of the MUC-1 C-ter fragment allowed this fragment to function as an oncogenic protein to shuttle transcription factors or co-factors

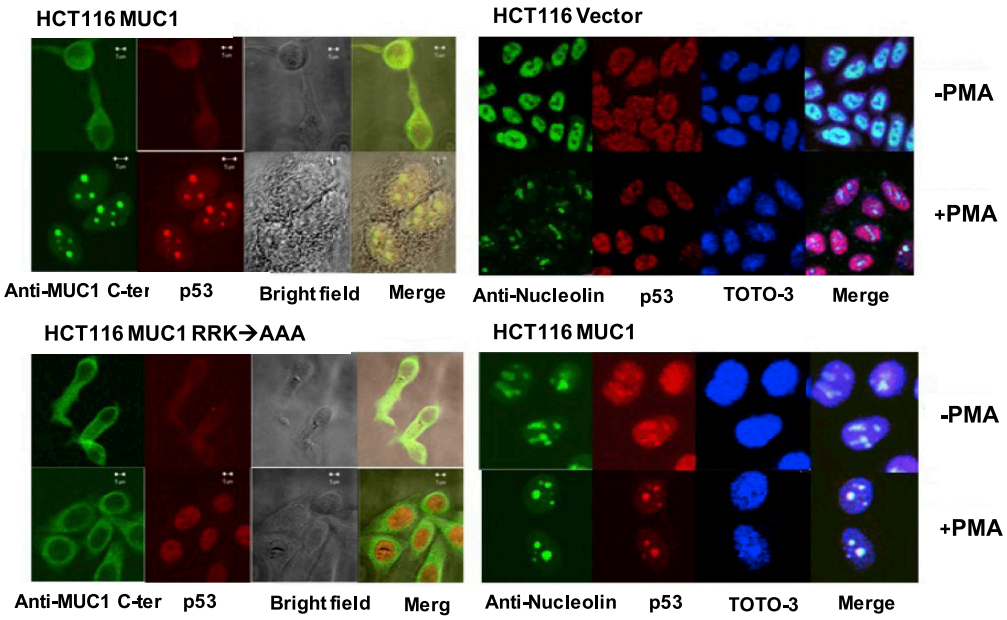

Figure 5. MMP-7-Mediated MUC-1-Dependent Nucleolar Assembly and p53 Nucleolus Trafficking

The assembly of the enlarged concentric nucleolus is an MUC-1 dependent on the PMA-treated HCT116 cell line. P53 significantly translocates into the nucleolus in the PMA-treated MUC-1-transfected HCT116 cell line. The immunofluorescence double staining for MUC-1 C-ter and p53 nucleolin indicate that both molecules are well colocalized in the nucleolus compartments, which are identified by immunostaining for nucleolin. In the absence of MUC-1, nucleolin assembly is not active and the MUC-1 with NLS mutation (RRK→AAA) mutant can abolish p53 translocating into nucleolus.

into the nucleolar compartment. Consequently, a transcriptional switch from RNA Pol type II transcription to RNA Pol type I transcription may take place in the nucleolus. In fact, enlarged concentric nucleoli were observed in most breast carcinoma cells but not in normal mammary glandular epithelial cells (Figure 4E right lower panel). Moreover, the activities of MMP-7 were associated with the enlargement of the concentric nucleolus (Figure 4E left upper panel). An enlarged nucleolar compartment may act as a molecular cage that harbors potent suppressors and forces active RNA pol type I-dependent transcription, which takes place in this subnuclear compartment, while segregating these factors from type II transcription. Accordingly, we investigated the ability of MUC-1 C-ter to shuttle tumor suppressor p53 into the nucleolus compartment. To recapitulate the role of MUC-1 shedding in the nucleolus assembly and sequestrating p53, the colorectal carcinoma cell line, HCT116, which MUC-1 and active MMP-7 is barely detectable was used to test the hypothesis that PMA stimulating MUC-1 shedding involved in p53 nucleolus translocation . The immunofluorescence double staining for MUC-1 C-ter and p53 was performed for the MUC-1 transfected cell lines, where HCT116 $^{MUC-1}$ was compared with the vector or NLS MUC-1 RRK→AAA mutant cell lines to investigate sub nucleus localization of p53 and MUC-1 C-ter in the PMA-induced active MUC-1 shedding. Interestingly, the enlarged nucleolus and MUC-1 C-ter nucleolus localization coincided in the PMA-stimulated HCT116^{MUC-1} cell line (Figure 5 left upper panel) not in the PMA-stimulated vector, mock-transfected, HCT116^{vector} cell lines or non-PMA-stimulated cells (Figure 5 right upper panel and left lower panel). More interestingly, the well colocalization of MUC-1 C-ter and p53 was observed in the enlarged concentric nucleolus-like sub-nucleus compartment in the PMA-stimulated HCT116^{MUC-1} cell line. The MUC-1$^{RRK→AAA}$ nucleus localization signal (NLS) mutant is defective in nucleus traffic even in the presence of PMA stimulation. The active MMP-7 can functionally shed NLS-mutant MUC-1 RRK→AAA and produce MUC-1 RRK→AAA C-ter; however, this MUC-1$^{RRK→AAA}$ C-ter loses the NLS and cannot enter the nucleus, accumulating in the peri nucleus membrane (Figure 5 left lower panel). P53 is localized in the nucleoplasm in the PMA-stimulated HCT116$^{MUC-1\ RRK→AAA}$ cell line (Figure 5, left lower panel). To validate that the enlarged concentric sub-nucleus compartment is nucleolus in the PMA-stimulated HCT116 $^{MUC-1}$ cells, anti-p53 and anti-nucleolin immunofluorescence double staining was performed. In the presence of MUC-1, PMA-stimulated MMP-7 shedding, p53 and MUC-1 C-ter were well co-localized in the RNA polymerase type I-dependent transcription nucleolus positive enlarged concentric sub-nucleus

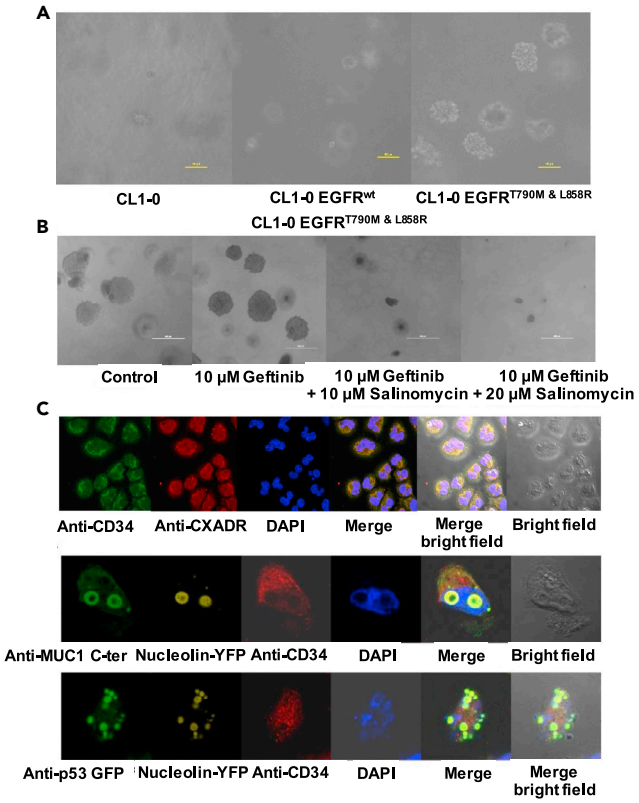

Figure 6. MUC-1 C-Ter and p53 Were Co-localized in Nucleolus of the CD34^{+} CXDR^{+} EGFR$^{L858R/T790M}$ CL1-0 Derived Lung CSCs

(A) Increasing the anchorage-independent growth capacity of the gefitinib-resistant EGFR$^{L858R/T790M}$ CL1-0 colonies in soft agar assay.

(B) Salinomycin can abolish the anchorage-independent growth abilities of EGFR$^{L858R/T790M}$ transfected CL1-0 cells in the presence of 10-μM gefitinib.

(C) The EGFR$^{L858R/T790M}$ CL1-0 small lung carcinoma cells selected colonies from soft agar assay were further transfected with plasmid nucleolin-YFP fusion constructs, and the stable EGFR$^{L858R/T790M}$ CL1-0/nucleolin-YFP cell colony was used to perform the immunostaining with anti-CXADR, and anti-CD34 Ab followed by labeling with anti-mouse-Texas Red fluorescence, anti-rabbit GFP, and nucleus was stained with DAPI. Both p53 and MUC-1 C-ter are localized in nucleolin by using anti-p53 polyclonal Ab, anti-MUC-1 C-ter (MUC-1-CD) Ab, anti-CXADR, and anti-CD34 Ab followed by labeling with the pair of anti-mouse GFP/anti-rabbit Texas Red, anti-mouse-Texas Red/anti-rabbit FITC fluorescence, and nucleus was stained with DAPI.

compartment in the PMA stimulated HCT116^{MUC-1} cells (Figure 5 right lower panel). In contrast, in the absence of MUC-1 and PMA stimulation, or PMA-stimulated HCT116$^{MUC-1\ RRK\rightarrow AAA}$ cells, the nucleolus appeared dispersed and p53 was mainly localized in the RNA polymerase type 1-dependent nucleus plasm (Figure 5 right upper and left lower panels).

MMP-7/MUC-1 C-Ter Mediates Intranucleolar Proteolytic Processing 35 kDa p53 in EGFR$^{L858R/T790M}$ CSCs

Because the expression of MMP-7 is upregulated through activating EGFR pathway (Figure 1F), the significantly enhanced anchorage-independent growth ability of EGFR constitutively active EGFR$^{L858R/T790M}$ CL1-0 small lung carcinoma cells was observed in the soft agar growth assay (Figure 6A). The selected soft agar growth colonies also exhibit suspension sphere growth capability, indicating the 10-μM gefitinib chemoresistant cancer-stem-cell-like phenotype (Figure 6B left two panels). The selected soft agar growth clones were positive for the immunofluorescent double staining with anti-CD34 and anti-CXADR (Figure 8C upper panel). The enlarged ringlike porous nucleolin (yellow) was also observed in the CD34-positive nucleolin-YFP vector-transfected EGFR$^{L858R/T790M}$ CL1-0 soft agar growth clones (Figure 8C middle panel).

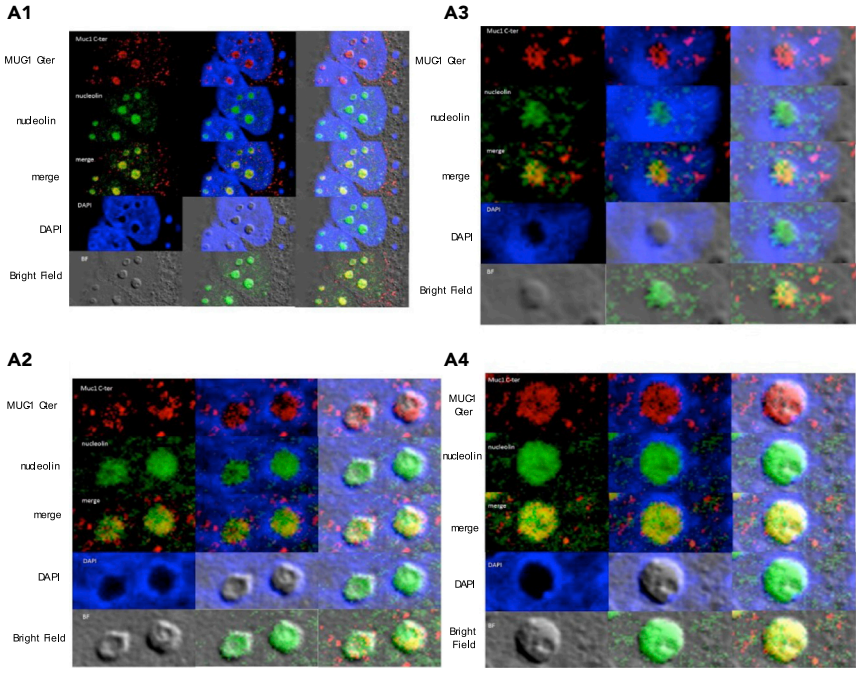

Figure 7. MUC-1 C-Ter Is Involved in Nucleolus Matrix Assembly and Regulates Nucleolar Structure in CD34^{+} EGFR$^{L858R/T790M}$ CL1-0-Derived CSCs

The MMP-7 upregulated expression EGFR constitutively active EGFR$^{L858R/T790M}$ CL1-0 small lung carcinoma cells selected from colonies from soft agar assay were further transfected with plasmid nucleolin-YFP fusion constructs, and the stable EGFR$^{L858R/T790M}$ CL1-0/nucleolin-GFP cell colonies were used to perform the immunostaining with anti-MUC-1 C-ter (MUC-1-CD) Ab.(A1–A4): Confocal microscopic analysis for immune-fluorescence staining for anti-MUC1 C-ter (MUC-1-CD) (Texas Red), nucleolin-YFP fusion protein expression (Green), and co-staining DAPI for nucleus chromosome (Blue). The sub-nucleus compartment colocalization of MUC1 C-ter (Red) with nucleolin (Green) in the DNA(DAPI) exclusive sub-nucleus compartment, nucleolus, (A1 is zoom out image and A2, A3, and A4 are zoom in images). The size and shape of nucleolus appear to be dependent on the relative amount of MUC-1 C-ter (Red) and nucleolin (Green) in the nucleolus. The complex of MUC-1 C-ter and nucleolin seem to be DNA (DAPI) exclusive and induce dome-like structure in the nucleus (see images of the DAPI merge with bright field), particularly in panel A3. In the lowest level of MUC-1 C-ter and nucleolin complex zone, the DNA clear zone starts to appear and the mosaic-architecture between MUC-1 C-ter (net-like in Red) and nucleolin (tetra-pod-like in Green) can be visualized.

The well-colocalized p53 with enlarged ringlike nucleolin was also observed in the clones (Figure 6C bottom panel).

The subcellular localization of nucleolin and MUC-1 C-ter was examined in the soft agar grown selected colonies of the EGFR constitutively active EGFR$^{L858R/T790M}$ CL1-0 small lung carcinoma cells. The nucleolar activities and morphology were visualized under confocal microscopy *in situ*; interestingly, the prominent enlarged nucleolus was observed (Figure 7A). The well colocalization between MUC-1 C-ter (Texas Red) and nucleolus (Green) indicated that MUC-1 C-ter translocated into the nucleolus compartment where chromosome DNA (DAPI/blue) are exclusive to the area (Figures 7A1–7A4). The size of the nucleolus is dependent on the amount of MUC-1 C-ter, which is proportional to the nucleolin intensity in mosaic architecture (Figures 7A3 and 7A4). MUC-1 C-ter forming a nucleolus matrix-like structure in the chromosome free zone where the active nucleolus assembly activities took place indicated through the nucleolin-YFP fusion protein localized (Figures 7A1–7A4). The well colocalization of nucleolin-YFP and anti-p53 (Texas Red) was also observed in the EGFR$^{858R/T790M}$ CL1-0 small lung carcinoma cells (Figures 8A1 and 8A2). We observed that p53 (Texas Red) is sequestrated inside the interesting bulky-ball shape nucleolus (nucleolin), which has not been reported before. It is implicated that this bulky-ball-like cage-shaped nucleolin could sequestrate p53 in the chromosome DNA exclusive zone (Figures 8A1 and 8A2). The physical contact between nucleolin and MUC-1 C-ter is confirmed by immunoprecipitation directly from nucleus isolation extracts by using anti-nucleolin antibodies followed by immunoblotting with anti-p53. The IP data strongly suggest that p53 can come into physical contact with nucleolin, but p53 undergoes further proteolytic

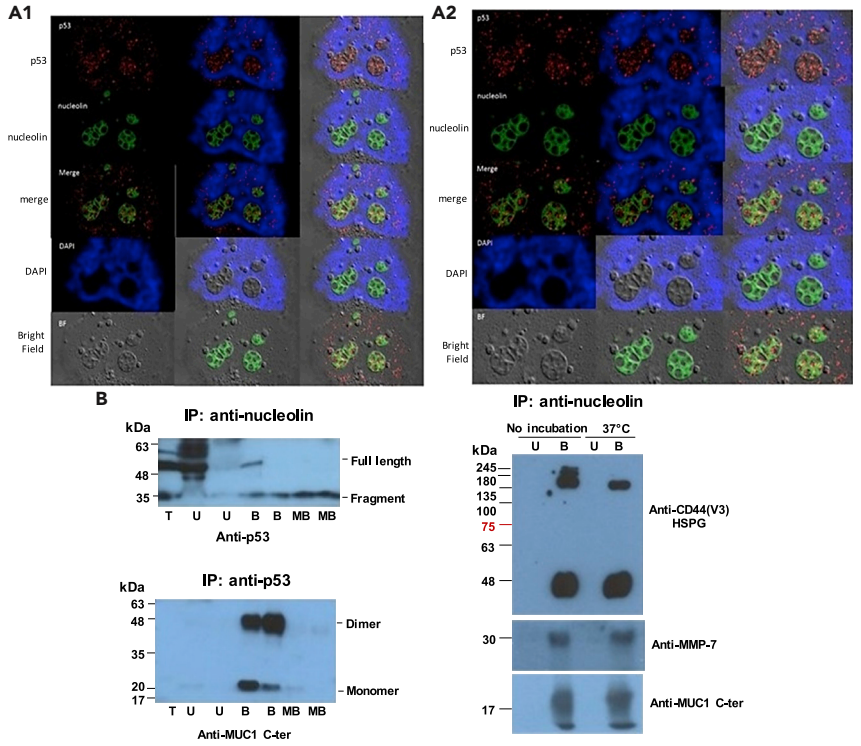

Figure 8. MMP-7 Mediates Proteolytic Processing p53 to 35 kDa Fragments in the Bulky-Ball-like Nucleolus of the CD34^{+} EGFR$^{L858R/T790M}$ CL1-0-Derived CSCs

The pcDNA p53 desRED and pcDNA nucleolin-YFP were co-transfected into floating sphere EGFR$^{L858R/T790M}$ CL1-0 CSC-like clones. Posttransfection 48 h, the cells were stained with DAPI to label nucleus and followed by confocal microscopic analysis.

(A1 and A2) Sub-nucleus compartment colocalization of p53 (Red) with nucleolin (green) in the DNA (DAPI) exclusive sub-nucleus compartment, nucleolus, (A1 zoom out and A2 zoom in). The enlarged nucleolus appears as a bulky-ball-shaped cage, nucleolin-YFP (in green). The structure is just like a "bulky-ball-cage" and the abundant p53 (Texas Red) sequestrates inside the nucleolin cage-like compartment.

(B) Immune-precipitation was performed directly from nucleus isolation extracts by using anti-nucleolin monoclonal Abs or anti-p53 monoclonal antibodies followed by western blot followed by immunoblotting with anti-p53, anti-MMP-7 (RM7C), anti-nucleolin, anti-CD44v3 mAb (R&D Systems), or anti-MUC-1 CD. U: Unbound; B Bound; MB: MicroBead

cleavage into ~35 kDa fragments, which indicates that p53 is not stable in the nucleolus compartment (Figure 8B, left upper panel). MUC-1 C-ter can also form a complex with nucleolin through IP experiment. The nucleolin-IP complex pulls down the MUC-1 C-ter monomer to not only around ~21 kDa but also ~42 kDa MUC-1 C-ter dimer (Figure 8B, left lower panel). These results indicate that MUC-1 C-ter dimer participates in the nucleolin complex during the nucleolus assembly. To investigate if MMP-7 is the putative protease involved in proteolytically cleaving p53 and producing 35 kDa fragments, first the nucleolus localization of MMP-7 in CSC-like cells was validated by co-transfecting the fluorescent tag fusion proteins expression constructs, pcDNA MMP-7 CFP and pcDNA nucleolin YFP, into floating sphere EGFR$^{L858R/T790M}$ CL1-0 CSC-like clone; interestingly, the well colocalization of MMP-7 CFP and nucleolin YFP in nucleolus observed indicate that MMP-7 potentially facilitates the proteolytic processing of nucleolar resident proteins (Figure 9A). To further investigate the idea that MMP-7 could proteolytically cleave p53 and generate 35 kDa fragments, the nucleolin complex is pulled down by using anti-nucleolin antibodies followed by immunoblotting with anti-MMP-7(RM7C), anti-CD44v3 mAb (R&D Systems), and anti-MUC-1 C-ter (Figure 8B right panel). MMP-7/CD44(V_3)HSPG complex existing in nucleolin IP complex implicate that MMP-7 translocates into the nucleolus compartment potentially forming a ternary complex with nucleolin and further incubating the anti-nucleolin/MMP-7/CD44v3 complex at 37°C can further proteolytically convert CD44v3 into the ~140 kDa and ~50 kDa fragments, which implicated that MMP-7 can proteolytically cleave CD44v3 (Figure 8B right upper panel) and also further proteolytic processing p53 generating 35 kDa fragments in the nucleolus compartment (Figure 8B left upper panel).

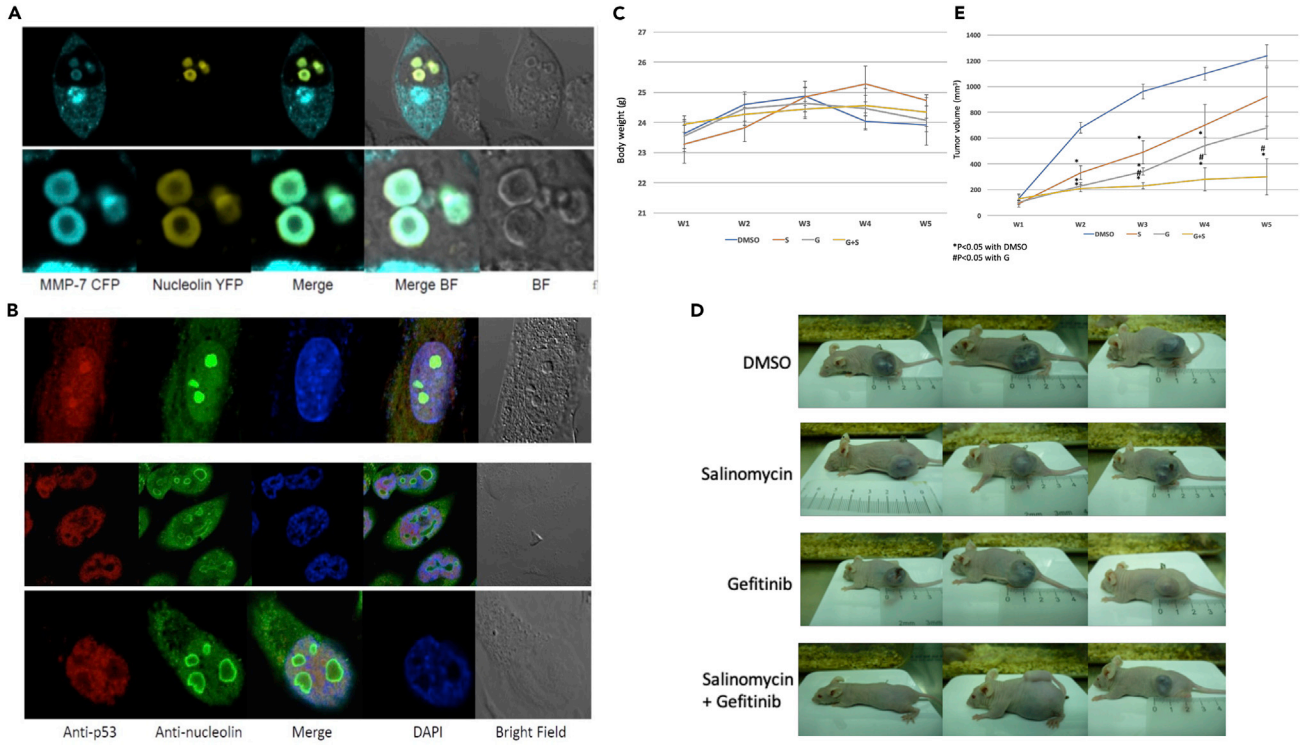

Figure 9. Salinomycin Disrupts Nucleolus and Releases Nucleolar p53 into Nucleoplasm Sensitizing CD34$^+$ EGFR$^{L858R/T790M}$ CL1-0 Derived CSCs to Gefitinib Treatment

(A) The localization of MMP7-CFP appears not only in the cell surface but also in the nucleolus compartment. Nucleolus localization of MMP-7 and proteolytic processing p53 by MMP-7 in the nucleolus of EGFR$^{L858R/T790M}$ CL1-0 CSC-like clones. (top panel) The fluorescent tag fusion proteins mammalian expression constructs, pcDNA MMP-7 CFP and pcDNA nucleolin YFP, were co-transfected into the floating sphere EGFR$^{L858R/T790M}$ CL1-0 CSC-like clones. Posttransfection 48 h, the cells were stained with DAPI to label nucleus and followed by confocal microscopic analysis, the colocalization of MMP-7 CFP and nucleolin YFP in porous-ring-like nucleolus were observed. The colocalization of MMP-7 CFP and nucleolin YFP were observed in the nucleolus compartments. The porous-ring-like nucleolus co-localized with MMP-7-CFP were observed in higher magnification. The major signal of nucleolin-YFP appears in the bulky-ball ring-like nucleolus is where the MMP-7 CFP also localized (bottom panel).

(B) Top panel: well colocalization of anti-p53 polyclonal-Ab-desRed and anti-nucleolin monoclonal Ab-GFP in the absence of salinomycin treatment. Middle and bottom panels: in the presence of salinomycin treatment, the enlarged nucleolin is disrupted and the nucleoplasm redistribution of p53 from nucleolus is observed. EGFR$^{L858R/T790M}$ CL1-0 cancer-stem-cell like cells are sensitive to the nucleolin-targeting drug salinomycin.

(C–E) Salinomycin promotes antitumor ability of gefitinib *in vivo*. Six-week-old BALB/c/nu mice were subcutaneously injected with 2 × 10^6 cells CL1-0 overexpressed double mutant EGFR single stable clone cells for 28 days then treated with DMSO (D), 5 mg/kg/day of salinomycin (S), 60 mg/kg/day of gefitinib (G), and combine treatment (G + S) for 28 days. (C) The body weight of experimental mice. (D) and (E) The mice with tumor were displayed and the quantitative results were shown. *p < 0.05 v.s. DMSO group; #p < 0.05 v.s. G group.

Because EGFR$^{L858R/T790M}$ CL1-0 small lung carcinoma cells are documented with a strong gefitinib chemo-resistant phenotype, potentially attributed to its sub-population with CSC phenotype, the disruption of the enlarged nucleolus could potentially be a novel therapeutic approach to overcome its chemoresistance and kill CSCs. To approach and justify this idea, the nucleolin-binding molecule, salinomycin, an anti-CSC agent, can suppress neuroblastoma CSC biomarker CD34 expression, induce CSC cell apoptosis, and reduce CD34$^+$ cell population via disrupting the interaction of NCL with the CD34 promoter (Wang et al., 2019). The treatment of salinomycin can abolish the anchorage-independent growth ability in soft agar and suspension growth capability of the EGFR$^{L858R/T790M}$ CL1-0 small lung carcinoma soft agar growth clones (Figure 6B). Salinomycin can disrupt the bulky-ball-like enlarged nucleolin and liberate p53 from nucleolus to nucleoplasm (Figure 9B middle and lower panels). The p53 nucleoplasm translocation from nucleolus could potentially sensitize CD44/CD34-positive CSC to apoptosis.

Salinomycin Promotes the Antitumor Ability of Gefitinib *In Vivo*

To consolidate the *in vitro* findings, the BALB/c/nu mice were subcutaneously injected with single stable cloned cell, CL1-0 overexpressed double mutant (DN) EGFR$^{T790M/L858R}$ for 28 days. The tumor-bearing

mice were treated with 60 mg/kg/d of gefitinib with or without 5 mg/kg/d of salinomycin by osmotic pump for further 28 days. There was no significant body weight decrease in the group of salinomycin treatment indicating no apparent toxicity observed (Figure 9C). The tumor volume was significantly increased on day 28 and the tumor growth inhibition ability of gefitinib was enhanced by co-treatment of salinomycin (Figures 9D and 9E). The results strongly suggest that salinomycin promotes the antitumor ability of gefitinib *in vivo*. The findings agree with the clinical trial of MUC-1 C-ter peptide dimer inhibitor (GO-203), the cell membrane penetrating peptide (R)9 CQCRRKN, demonstrating both potently attenuate the lenalidomide resistance for multiple myeloma and the gefitinib resistant for small cell lung carcinoma cells. The anti-chemotherapy resistance underlying mechanism for the MUC-1 C-ter dimmer inhibitor G0-203 could attribute to the actions of blocking the dimmer formation of MUC-1 C-ter and further intervening with the nucleolus translocations of p53.

Concluding that the dimmer of MUC-1 C-ter facilitates p53 nucleolus traffic and participates in nucleolus matrix assembly could confirm the capability of gefitinib chemoresistance of the $CD34^{+}$ $EGFR^{L858R/T790M}$ cancer stem-like cells. Interestingly, GO-203, an MUC-1 C-ter dimmer inhibiting peptide, can sensitize the multiple myeloma cells to lenalidomide, a small lung cell carcinoma, to gefitinib, and breast carcinoma cell to tamoxifen and cisplatin treatments. The diminishing multiple chemoresistances of the GO-203 peptide implicates the underlying potential molecular mechanism of GO-203 peptide targets to stem cell pools. The action of salinomycin to kill the gefitinib-resistant $EGFR^{L858R/T790M}$ CL1-0 CSC-like cells could attribute to the capability of disrupting the nucleolus of CSC cells.

DISCUSSION

MMP-7 Functions as a Novel Regulatory Effector for Rewiring the p53 Signal Transduction Pathway through Proteolysis

The results of the present study provide evidence for a novel function of MMP-7 in modulating the p53 signaling pathway. Our findings demonstrate that MMP-7 is responsible for targeting p53 to the nucleolus. The treatment of HCT116 colon cancer cells with PMA was associated with the activation of MMP-7 and consequent nucleolar localization of p53 (Figure 5). Conversely, the inhibition of MMP-7 by TIMP-3 or SC44463 blocked this response. Moreover, our results show that recombinant MMP-7 induced the same redistribution of p53 from the nucleus plasm to the nucleolus, which constitutes direct evidence (Figure 5). Similar to β-catenin, γ-catenin is expressed in adherent junctions, where it links E-cadherin to the actin cytoskeleton via α-catenin. The redistribution of Wnt signaling molecule, γ-catenin from membrane to nucleolus is MUC-1 C-ter dependent in the presence of heregulin (Li et al., 2003c). The cell membrane would subvert E-cadherin function, an event that is associated with the loss of cell-cell adhesion and invasion (Perl et al., 1998; Vleminckx et al., 1991). Thus, the aberrant expression of MMP-7 via the activation of the Wnt pathway in human tumors could, in turn, contribute to the malignant phenotype via the dysregulation of p53 signaling in the nucleus (Figure 5).

MMP-7 Is a Facultative Enzyme to Shed MUC-1 and Liberate the Dimmer of MUC-1 C-Ter

It has been known that MUC-1 C-ter functions as an oncogene (Nath and Mukherjee, 2014). In cancer cells, MUC1 C-ter directly associates with many growth factors such as EGF receptor (EGFR) upon stimulation. MUC-1 C-ter can be translocated into the nucleus where it binds to cyclin D1 (CCND1) and v-myb myeloblastosis viral oncogene homolog-like 2 (MYBL2) promoters. It enables G1/S phase gene expression (Bitler et al., 2010) and cancer cell proliferation (Sahraei et al., 2012).

MMP-7 functions as an MUC-1 sheddase. Secreted MMP-7 is normally found at the apical borders of glandular epithelial cells, where it is tethered to the cell surface by binding to heparan sulfate proteoglycans (Yu and Woessner, 2000). In the intestinal mucosa, MMP-7 activates the pro-α-defensin family of antimicrobial peptides (Wilson et al., 1999). MMP-7 also generates soluble Fas ligand (Mitsiades et al., 2001; Powell et al., 1999), processes the HB-EGF precursor (Yu et al., 2002), and mediates the shedding of syndecan-1 (Li et al., 2002). Other studies have supported the involvement of MMP-7 in the migration of the epithelium from the damaged mucosa of the respiratory and intestinal tracts (Dunsmore et al., 1998; Saarialho-Kere et al., 1996). Moreover, MMP-7 null mice exhibit defects in wound repair (Parks and Shapiro, 2001), but they are also protected against bleomycin-induced pulmonary damage due to the impaired transepithelial migration of neutrophils to sites of injury (Li et al., 2002). These findings have collectively supported diverse functions for MMP-7 in tissue defense, repair, and inflammation.

The *in vitro*, *in silico*, and cell culture experimental results (Figures 1 and 2) demonstrated that the MUC-1 C-ter SEA domain can bind to mature MMP-7, and the Gly-Ser loop (K111FRPG↓SVVV119) (Pelaseyed et al., 2013) of the SEA domain can insert into the active center of MMP-7 and thus potentially be cleaved at Gly115-Ser116 sites (Figures 2A and 2B). The ability of MMP-7 to function as a putative SEA domain shedding protease, in addition to the unknown mechanism underlying conventional auto-proteolysis, is a novel finding (Macao et al., 2006). The thermally unstable Gly-Ser-loop (Pelaseyed et al., 2013) may provide a position that is easily attacked by the active site of mature MMP-7, and the MMP-7 inhibitor SC44463 (Edman et al., 2011; Yu et al., 2012) can prevent the production of cleaved MMP-7 C-ter (Figures 1D and 1E). The present results define a novel function for MMP-7 in the proteolytic processing of the SEA domain of MUC-1. Mucins are a family of heavily glycosylated proteins that are secreted or tethered to the cell surface by a transmembrane domain. Secreted mucins form a protective barrier that serves as a defense against damage to the glandular epithelium. The transmembrane mucins also contribute to this defense barrier. MMP-7 can interact with and cleave Gly-Ser sites within the loop of the SEA domain of full-length MUC-1 *in vitro* through immunoprecipitation by using anti-MUC-1 N-terminal antibodies from ZR-75-1 cell extract (Figure 1D). However, to test whether MMP-7 can also cleave the SEA domain of the MUC 1-ECD-Fc fusion protein (Figure 1E), MUC 1-ECD-Fc fusion protein IP with anti-Fc antibodies and further digested with *E. coli*-derived purified recombinant MMP-7 also cleaved the SEA domain at a novel PF cleavage site in the monomer form. Thus, cleavage of the extracellular region of the MUC 1 C-ter fragment, which forms a heterodimer with the N-ter fragment, provides a mechanism for the shedding of the MUC-1 ectodomain by MMP-7, which is possibly a physiological stress response to the external environment to enhance physical protection. Moreover, the cleavage of MUC-1 by MMP-7 may also contribute to the transduction of stress signals to the interior of the cell.

MMP-7-induced cleavage of MUC-1 is responsible for nucleolar targeting of γ-catenin. MUC-1 interacts with EGFR and ErbB2-4 in epithelial cells (Li et al., 2003c; Schroeder et al., 2001). Other work has shown that HRG and PMA induce the cleavage of the ErbB4 ectodomain (ECD) by tumor necrosis factor alpha converting enzyme (TACE) and that the cytoplasmic domain translocates to the nucleus following intramembrane proteolysis (Ni et al., 2001; Zhou and Carpenter, 2000). After ligand binding, EGFR may undergo processing similar to the nuclear translocation of the cytoplasmic domain (Lin et al., 2001). Studies of uterine epithelial cells have suggested that the MUC-1 ECD can also be shed by TACE; however, the location of this cleavage (N-ter or C-ter) and the ability of TACE to induce the translocation of MUC-1 to the nucleus are unknown (Thathiah et al., 2003). In our studies, CHO cells expressing the MUC-1 (ECD)-Fc fusion protein exhibited high levels of functional TACE (Borrell-Pages et al., 2003). However, the low to undetectable levels of cleaved MUC-1 (ECD)-Fc indicated that a protease other than TACE was responsible for the shedding of the MUC-1 N-ter fragment. Indeed, our results showed that MMP-7 cleaved the MUC-1 C-ter fragment and that this processing specifically initiated the targeting of MUC-1 C-ter to the nucleolus (Figure 3).

Furthermore, the necessity of both MMP-7 and MUC-1 for the targeting of p53 to the nucleolus further supports the functional significance of the MMP-7-induced cleavage of MUC-1 C-ter. These findings indicate that MUC-1 C-ter may function as a nucleolar shuttle for p53 after the MMP-7-mediated processing of MUC-1 C-ter at the cell membrane (Figure 5). The transcription and processing of rRNAs is a major function of the nucleolus that reflects the increase in protein synthesis during cell growth and metastasis (Pederson, 1998). The present study showed that the nucleolar targeting of MUC-1 C-ter was associated with the formation of distinct, enlarged nucleolus in both ZR-75-1 and HCT116 cells (Figure 3). Changes in nucleolar structure have long been recognized as a hallmark of cellular transformation and may involve the deregulation of ribosomal proteins (Ruggero and Pandolfi, 2003). Accordingly, MUC-1 C-ter is physically associated with nucleolin (Figure 8B right lower panel) and may consequently affect the function of nucleolin in the regulation of ribosome biogenesis and maturation. However, further studies are needed to define the nature of the interaction between MUC-1 C-ter and nucleolin.

MMP-7-MUC-1 C-ter signaling disrupts mammary acinar structures. The MUC-1 C-ter fragment interacts with the Wnt pathway by binding to β-/γ-catenin and by functioning as a substrate for GSK3β-mediated phosphorylation (Li et al., 1998; Yamamoto et al., 1997). MUC-1 also interacts with members of the ErbB family (Li et al., 2003c; Schroeder et al., 2001), which supports that MUC-1 plays a role in integrating signals from activated tyrosine kinase receptors with those of the Wnt pathway. Nevertheless, the positioning of MUC-1 C-ter along the apical borders of secretory epithelial cells would preclude interactions with growth factor receptors expressed on basolateral borders. However, the integrity of tight junctions between

neighboring cells, and therefore polarity, is lost as part of the repair program in response to stress (Vermeer et al., 2003). In addition, as a consequence of the loss of polarity, HRG is made accessible for the activation of ErbB2 and, thereby, the repair of epithelial integrity (Vermeer et al., 2003). Our results demonstrate that HRG/or PMA-induced signaling is also associated with the activation of MMP-7-MUC-1 C-ter signaling and that this pathway is of importance to the loss of polarity associated with the epithelial-mesenchymal transition (Figures 1B and 4E).

MMP-7 has also been implicated in mammary and gastrointestinal tumorigenesis (Crawford et al., 1999; Rudolph-Owen et al., 1998; Wilson et al., 1997; Witty et al., 1994). In addition, evidence that (1) a dominant-negative MMP-7 blocks the growth of ZR-75-1 foci as domes, (2) the knock-down of MUC-1 blocks ZR-75-1 multilayered foci, and (3) γ-catenin contributes to the formation of RK3E rat epithelial cell foci (Kolligs et al., 2000) collectively suggested that MMP-7-MUC-1 C-ter-p53 signaling might be important for the anchorage-independent growth and 3-dimensional cultures of epithelial cells. Mammary acinar units consist of polarized epithelial cells that surround a hollow lumen, but epithelial damage and the development of carcinomas disrupt these structures. Notably, the activation of ErbB2 reinitiates proliferation in preformed mammary epithelial acini and generates complex multi-acinar structures that are associated with early stage carcinomas (Muthuswamy et al., 2001). The loss of acinar structure is also associated with reduced levels of luminal apoptosis (Muthuswamy et al., 2001). The present results demonstrate that MMP-7 induced complex multi-acinar structures with filled lumens and that MUC-1 was necessary for this response (Figure 6). Although our findings also showed that HRG activated MMP-7, an ErbB2-MMP-7-MUC-1 signaling pathway may contribute to the effects of ErbB2 activation on the disruption of mammary acinar structures (Muthuswamy et al., 2001). Because HRG activates ErbB2 in response to epithelial damage (Vermeer et al., 2003), the MMP-7-MUC-1 pathway may physiologically function in the repair process. Indeed, MUC-1 may function as a sensor that, in response to a loss of polarity, transduces stress signals to the nucleus. Alternatively, the overexpression of MMP-7 and MUC-1 in epithelia could contribute to the dysregulation of this pathway and thereby the induction of the epithelial-mesenchymal transition and carcinogenesis (Polakis, 2000) (Figures 4D and 4E).

MUC-1 C-ter participates in AgNOR and the cryptic nucleolus-targeting shuttle molecule. The novel finding that MUC-1 C-ter participates in AgNOR and the assembly of the nucleolar matrix suggested that the cell surface receptor MUC-1 could release cryptic bioactive fragments via proteolysis to regulate the nuclear sub-compartment protein nucleolin. Via this mechanism, cells can sense extracellular cues to orchestrate ribosome biogenesis and modulate nucleolar assembly (Figures 4 and 5).

MUC-1 C-Ter Functions as a Nucleolus Shuttle Molecule for Tumor Suppressor, p53, and Facilitates Intra-nucleolus Proteolytic Processing p53 by MMP-7

The MUC-1 C-ter inducing a unique, porous, bulky-ball-shaped cage-like nucleolus could function as a nucleus molecular "garage" for the tumor suppressor, p53, to segregate transcription factors from their target promoters confirming another level of fine-tuning of protein expression in CSCs (Figures 5 and 6). The intra nucleolus degradation of p53 to generate 35 kDa p53 fragment prompts an interesting idea that the nucleolus could play another special role as a novel sub-nucleus protein degradation compartment for clearing the tumor suppressor p53 (Figure 8). The proteolytic processing of MUC-1 by MMP-7 releases MUC-1 C-ter to facilitate the shuttling of p53 into the nucleolus, which suggests that many cryptic nucleolar shuttles could be liberated by these proteolytic actions to respond to changes in the extracellular and cell surface compartments, such as epithelial-mesenchymal transition and CSC transformation.

Several findings support the conclusion that MMP-7 and MUC-1 cooperate to translocate the tumor suppressor p53 into the nucleolar compartment and also to participate in the assembly of the nucleolus. First, overexpression of MUC-1 is associated with an enlarged nucleolus; second, MMP-7 overexpression strongly correlates with a distinct, enlarged nucleolus; third, MUC-1 and MMP-7 are co-expressed in cells containing enlarged nucleoli; and fourth, MUC-1, CD44v3 (Epican), nucleolin, MMP-7, and nucleostemin are documented biomarkers for cancer and stem-like cancer cells. Therefore, we hypothesized that MMP-7-mediated post-translational proteolytic processing of MUC-1 releases MUC-1 C-ter fragments that can translocate into the nucleolus and participate in the assembly of the nucleolar matrix. Moreover, this proteolytic MUC-1 C-ter fragment can also facilitate the targeting of bio-active molecules to shuttle MUC-1 C-ter/MMP-7/p53 into the nucleolus and further sequester them from their substrates and also further proteolytic processing p53 into 35 kDa fragments. In addition to ribosome biogenesis and protein

synthesis, a novel biological function has been associated with this sub-nuclear compartment, the nucleolus, which functions as an intra-nucleolar MMP-7-mediated protein degradation compartment and generates the novel p53-derived proteolytic fragments functioning as the transcriptional switch for tumor suppressor protein, p53 (Figures 8 and 9A).

Salinomycin Disrupts Bulky-Ball-like Nucleolus Inducing SCS Apoptosis

Interestingly, upregulation of MUC-1 and CD44 expression is associated with CSC transformation, while several CSC-associated antigens, such as CD34 and CXADR, detected in the $EGFR^{L858R/T790M}$ CL1-0 soft agar growth selected colonies implicates that MUC1 and CD44HSPG(v3)/MMP-7 could play a critical role in CSC transformation (Figures 6, 7, and 9). In order to demonstrate the CSC properties of the soft agar grown colonies of the sub-population of EGFR constitutively active $EGFR^{L858R/T790M}$ CL1-0 small lung carcinoma cells, anti-CD34 immunofluorescence was co-stained with anti-p53 and anti-MUC-1 C-ter in the nucleolin-YFP transfected $EGFR^{L858R/T790M}$ CL1-0 CSC-like cells (Figure 6C). The well colocalization of anti-MUC-1 C-ter and anti-p53 activities in the bulky-ball-like nucleolus was observed (Figure 6C).

The gefitinib-resistant $EGFR^{L858R/T790M}$ CL1-0 small lung carcinoma cells are potentially attributed to their sub-population with a CSC-like phenotype (Figure 6A), where the disruption of the enlarged nucleolus could be potentially a novel therapeutic approach to overcome its chemoresistance and kill the CSC-like sub-population. To investigate this idea, the nucleolin-binding molecule, salinomycin, which can suppress neuroblastoma CSC biomarker CD34 expression and induce CSC cell apoptosis (Wang et al., 2019), was used to disrupt the nucleolus and abolish the anchorage-independent growth ability and suspension growth capability (Figure 6B). The nucleolus plays an important role in regulating p53 stability and maintaining the self-renewal for embryonic stem cells (Yang et al., 2011). In our studies, nucleolin can facilitate proteolytic processing p53 to 35 kDa fragments through the MMP-7-CD44v3 complex (Figure 8 B left upper panel). The 35 kDa p53 could be involved in a transcriptional switch for CSC lineage differentiation. The systematic analysis for the actions of these 35 kDa fragments will be revealed in the near future. MUC-1 C-ter-mediated enlarged bulky-ball-like nucleolus is a hallmark of chemotherapy-resistant small lung CSCs. To test the ideal that the bulky-ball-like nucleolin can contribute to CSC chemoresistance, the nucleolin-binding chemical compound, salinomycin, was used to disrupt the bulky-ball-like enlarged nucleolin and liberate p53 from nucleolus to nucleoplasm and potentially sensitize the $CD44^{+}CD34^{+}$CSC cells to apoptosis pathway (Figure 9B). The findings of p53 co-IP with MUC-1 C-ter dimers from the nucleus extracts of the $CD44^{+}CD34^{+}EGFR^{L858R/T790M}$ CSC cells agree with the clinical trial of MUC-1 C-ter dimer inhibitor (GO-203), the cell membrane penetrating peptide (R)9-CQCRRKN, demonstrating both potently attenuate the lenalidomide resistance for multiple myeloma and the gefitinib resistant for small cell lung carcinoma cells (Yin et al., 2017). The anti-chemotherapy resistance underlying mechanism for the MUC-1 C-ter dimmer inhibitor GO-203 could be attributed to the actions of blocking the dimmer formation of MUC-1 C-ter and further oblate the nucleolus translocations of p53.

Co-immunoprecipitating the dimmer of MUC-1 C-ter with p53 implicates that the dimer of MUC-1 C-ter could co-transport with p53 into the nucleolus (Figure 8B) and also participate in nucleolus matrix assembly attributed to the capability of gefitinib-chemoresistant $CD44^{+}CD34^{+}EGFR^{L858R/T790M}$ CSCs. Interestingly, G0-203, MUC-1 C-ter dimmer inhibiting peptide, can sensitize small lung cell carcinoma to gefitinib breast carcinoma cell to tamoxifen and cisplatin treatments, implicating that the GO-203 peptide could target the CSC pool that exhibits the chemotherapy resistance (Hasegawa et al., 2015).

In summary, MMP-7 mediated the shedding of MUC-1 to release a cryptic oncogenic nucleolar shuttle, MUC-1 C-ter, which can mediate the nucleolar translocation of p53. The current hypothesis is that MUC-1 C-ter, an oncogenic nucleolus shuttle protein, can modulate signaling pathways that are involved in re-wiring p53 signaling and proteolytic processing p53 to 35 kDa, which potentially drives CSC transformation (Figure 8). MUC-1 C-ter were also reported to be able to suppress the p53 pathway and to induce OCT4, SOX-2, KLF4, and MYC expression and to regulate cancer cell lineage plasticity (Yamashita et al., 2020). In another aspect, MUC-1 C-ter was reported to suppress p53 responsive gene transcription, and downregulating p21 and Bax expression confirms the resistance to genotoxic drugs such as cisplatin and etoposide (Wei et al., 2005). These evidence implicate the possible hypothesis that MUC-1 C-ter can not only suppress p53 but also potentially transcriptionally switch to drive cancer cells to CSC lineage differentiation and confirm the chemotherapy resistance. MUC-1 C-ter was reported to be oncoprotein, which facilitate multiple hallmarks of cancer cells, including drug resistance and CSC transformation; accordingly, the detailed

cellular mechanisms are revealed in this study: intranucleolus proteolytic processing p53 to 35 kDa fragments by MMP-7. The putative role of p53-derived 35 kDa fragments were documented to correlate to the anti-apoptotic effects against genotoxic insults (Okorokov and Milner, 1997). The hypothesis is that 35 kDa fragments could also potentially participate in the transcriptional switch toward CSC differentiation. Although other works have demonstrated that MUC-1 C-ter can regulate p53 signaling through silencing or a molecular switch (Wei et al., 2005 and Yamashita et al., 2020), our works bridge the detailed cellular mechanism from the cell surface shedding MUC-1 to liberate MUC-1 C-ter for shuttling p53 into the nucleolus to facilitate intra-nucleolar proteolytic processing p53 to 35 kDa fragments that open another new research avenue to address the putative role of p53 35 kDa fragments in rewiring the p53 signaling in the CSCs lineage differentiation in the near future. The findings of this study provide important new insights into the nucleolar post-translational proteolytic modification for rewiring p53 signaling in chemotherapy-resistant CSCs as well as highlight targets for cancer therapeutics.

Limitations of the Study

The detailed molecular mechanism underlying the action of nucleolus degrading p53 to 35 kDa in regulating cancer stem cell lineage differentiation and chemotherapy resistance has not been elucidated in this study. The amount of data for this study is considerably huge and we intend to study the p35 kDa p53 in more detail in the near future.

Resource Availability

Lead Contact

Further information and requests for resources should be directed to and will be fulfilled by the Lead Contact, Wei-hsuan Yu (whyu2004@ntu.edu.tw).

Materials Availability

All unique/stable reagents generated in this study are available from the Lead Contact with a completed Materials Transfer Agreement.

Data and Code Availability

All data supporting the findings of this study are included in the article and its Supplemental Information or are available from the corresponding authors on request.

METHODS

All methods can be found in the accompanying Transparent Methods supplemental file.

SUPPLEMENTAL INFORMATION

Supplemental Information can be found online at https://doi.org/10.1016/j.isci.2020.101600.

ACKNOWLEDGMENTS

The authors thank Dr. Joan Brugge for the MCF-10A cells and Ms. Eva Lin for providing assistance with the MCF10A mammary acinar cultures. The authors also thank Ms. Khanin Z. Yu for the technical assistance and Mr. Euni Wu for language editing of the manuscript. In addition, we are grateful to Ms. Hwa-man Shu for the excellent confocal microscopy technical support and the College of Medicine of the National Taiwan University for use of the confocal microscopy image core facility. This work was supported by the Ministry of Science and Technology of Taiwan (NSC-94-2320-B-002-120 to W.-H.Y.) and Corbett Estate Fund for Cancer Research (#62285), USA (E.W.).

AUTHOR CONTRIBUTIONS

W. H. Y. conceived the project and supervised its execution. W. H. Y., E. W., and Y. Q. L. designed the experiments, analyzed the data, and wrote the manuscript. W. H. Y., W. H. K., and H. S. Y. performed the experiments. H. H. H. and C. J. Y. conduct rodent xenograft and drug treatment. P. T. H. performed the bioinformatics and structural analyses. D. Q. helped with analyzing data and editing the manuscript. All authors discussed the results and provided comments on the manuscript.

DECLARATION OF INTERESTS

The authors declare no competing interests.

Received: February 18, 2020
Revised: April 21, 2020
Accepted: September 18, 2020
Published: October 23, 2020

REFERENCES

Behrendtsen, O., and Werb, Z. (1997). Metalloproteinases regulate parietal endoderm differentiating and migrating in cultured mouse embryos. Dev. Dyn. *208*, 255–265.

Bergers, G., Brekken, R., McMahon, G., Vu, T.H., Itoh, T., Tamaki, K., Tanzawa, K., Thorpe, P., Itohara, S., Werb, Z., and Hanahan, D. (2000). Matrix metalloproteinase-9 triggers the angiogenic switch during carcinogenesis. Nat. Cell Biol. *2*, 737–744.

Bergers, G., and Coussens, L.M. (2000). Extrinsic regulators of epithelial tumor progression: metalloproteinases. Curr. Opin. Genet. Dev. *10*, 120–127.

Bharti, A.K., Olson, M.O., Kufe, D.W., and Rubin, E.H. (1996). Identification of a nucleolin binding site in human topoisomerase I. J. Biol. Chem. *271*, 1993–1997.

Bitler, B.G., Goverdhan, A., and Schroeder, J.A. (2010). MUC1 regulates nuclear localization and function of the epidermal growth factor receptor. J. Cell Sci. *123*, 1716–1723.

Bode, W., Grams, F., Reinemer, P., Gomis-Ruth, F.X., Baumann, U., McKay, D.B., and Stocker, W. (1996). The metzincin-superfamily of zinc-peptidases. Adv. Exp. Med. Biol. *389*, 1–11.

Borrell-Pages, M., Rojo, F., Albanell, J., Baselga, J., and Arribas, J. (2003). TACE is required for the activation of the EGFR by TGF-alpha in tumors. EMBO J. *22*, 1114–1124.

Carmo-Fonseca, M. (2015). Assembly of the nucleolus: in need of revision. EMBO J. *34*, 2731–2732.

Cornelius, L.A., Nehring, L.C., Harding, E., Bolanowski, M., Welgus, H.G., Kobayashi, D.K., Pierce, R.A., and Shapiro, S.D. (1998). Matrix metalloproteinases generate angiostatin: effects on neovascularization. J. Immunol. *161*, 6845–6852.

Crawford, H.C., Fingleton, B.M., Rudolph-Owen, L.A., Goss, K.J., Rubinfeld, B., Polakis, P., and Matrisian, L.M. (1999). The metalloproteinase matrilysin is a target of beta-catenin transactivation in intestinal tumors. Oncogene *18*, 2883–2891.

Crawford, H.C., Scoggins, C.R., Washington, M.K., Matrisian, L.M., and Leach, S.D. (2002). Matrix metalloproteinase-7 is expressed by pancreatic cancer precursors and regulates acinar-to-ductal metaplasia in exocrine pancreas. J. Clin. Invest. *109*, 1437–1444.

Deisenroth, C., and Zhang, Y. (2010). Ribosome biogenesis surveillance: probing the ribosomal protein-Mdm2-p53 pathway. Oncogene *29*, 4253–4260.

Dunsmore, S.E., Saarialho-Kere, U.K., Roby, J.D., Wilson, C.L., Matrisian, L.M., Welgus, H.G., and Parks, W.C. (1998). Matrilysin expression and function in airway epithelium. J. Clin. Invest. *102*, 1321–1331.

Eckhard, U., Huesgen, P.F., Schilling, O., et al. (2016). Active site specificity profiling of the matrix metalloproteinase family: Proteomic identification of 4300 cleavage sites by nine MMPs explored with structural and synthetic peptide cleavage analyses. Matrix Biol. *49*, 37–60.

Edman, K., Furber, M., Hemsley, P., Johansson, C., Pairaudeau, G., Petersen, J., Stocks, M., Tervo, A., Ward, A., Wells, E., and Wissler, L. (2011). The discovery of MMP7 inhibitors exploiting a novel selectivity trigger. ChemMedChem *6*, 769–773.

Engsig, M.T., Chen, Q.J., Vu, T.H., Pedersen, A.C., Therkidsen, B., Lund, L.R., Henriksen, K., Lenhard, T., Foged, N.T., Werb, Z., and Delaisse, J.M. (2000). Matrix metalloproteinase 9 and vascular endothelial growth factor are essential for osteoclast recruitment into developing long bones. J. Cell Biol. *151*, 879–889.

Fonseca, N.A., Rodrigues, A.S., Rodrigues-Santos, P., Alves, V., Gregorio, A.C., Valerio-Fernandes, A., Gomes-da-Silva, L.C., Rosa, M.S., Moura, V., Ramalho-Santos, J., et al. (2015). Nucleolin overexpression in breast cancer cell sub-populations with different stem-like phenotype enables targeted intracellular delivery of synergistic drug combination. Biomaterials *69*, 76–88.

Gendler, S., Taylor-Papadimitriou, J., Duhig, T., Rothbard, J., and Burchell, J. (1988). A highly immunogenic region of a human polymorphic epithelial mucin expressed by carcinomas is made up of tandem repeats. J. Biol. Chem. *263*, 12820–12823.

Hasegawa, M., Sinha, R.K., Kumar, M., Alam, M., Yin, L., Raina, D., Kharbanda, A., Panchamoorthy, G., Gupta, D., Singh, H., et al. (2015). Intracellular targeting of the oncogenic MUC1-C protein with a novel GO-203 nanoparticle formulation. Clin. Cancer Res. *21*, 2338–2347.

Hernandez-Verdun, D., and Roussel, P. (2003). Regulators of nucleolar functions. Prog. Cell Cycle Res. *5*, 301–308.

Hooper, N.M., Karran, E.H., and Turner, A.J. (1997). Membrane protein secretases. Biochem. J. *321* (Pt 2), 265–279.

Hsu, T.I., Lin, S.C., Lu, P.S., Chang, W.C., Hung, C.Y., Yeh, Y.M., Su, W.C., Liao, P.C., and Hung, J.J. (2015). MMP7-mediated cleavage of nucleolin at Asp255 induces MMP9 expression to promote tumor malignancy. Oncogene *34*, 826–837.

Kolligs, F.T., Kolligs, B., Hajra, K.M., Hu, G., Tani, M., Cho, K.R., and Fearon, E.R. (2000). gamma-catenin is regulated by the APC tumor suppressor and its oncogenic activity is distinct from that of beta-catenin. Genes Dev. *14*, 1319–1331.

Kryczka, J., Stasiak, M., Dziki, L., Mik, M., Dziki, A., and Cierniewski, C. (2012). Matrix metalloproteinase-2 cleavage of the beta1 integrin ectodomain facilitates colon cancer cell motility. J. Biol. Chem. *287*, 36556–36566.

Kufe, D., Inghirami, G., Abe, M., Hayes, D., Justi-Wheeler, H., and Schlom, J. (1984). Differential reactivity of a novel monoclonal antibody (DF3) with human malignant versus benign breast tumors. Hybridoma *3*, 223–232.

Li, Q., Park, P.W., Wilson, C.L., and Parks, W.C. (2002). Matrilysin shedding of syndecan-1 regulates chemokine mobilization and transepithelial efflux of neutrophils in acute lung injury. Cell *111*, 635–646.

Li, Y., Bharti, A., Chen, D., Gong, J., and Kufe, D. (1998). Interaction of glycogen synthase kinase 3beta with the DF3/MUC1 carcinoma-associated antigen and beta-catenin. Mol. Cell. Biol. *18*, 7216–7224.

Li, Y., Chen, W., Ren, J., Yu, W.H., Li, Q., Yoshida, K., and Kufe, D. (2003a). DF3/MUC1 signaling in multiple myeloma cells is regulated by interleukin-7. Cancer Biol. Ther. *2*, 187–193.

Li, Y., Kuwahara, H., Ren, J., Wen, G., and Kufe, D. (2001a). The c-Src tyrosine kinase regulates signaling of the human DF3/MUC1 carcinoma-associated antigen with GSK3 beta and beta-catenin. J. Biol. Chem. *276*, 6061–6064.

Li, Y., Liu, D., Chen, D., Kharbanda, S., and Kufe, D. (2003b). Human DF3/MUC1 carcinoma-associated protein functions as an oncogene. Oncogene *22*, 6107–6110.

Li, Y., Ren, J., Yu, W., Li, Q., Kuwahara, H., Yin, L., Carraway, K.L., 3rd, and Kufe, D. (2001b). The epidermal growth factor receptor regulates interaction of the human DF3/MUC1 carcinoma antigen with c-Src and beta-catenin. J. Biol. Chem. *276*, 35239–35242.

Li, Y., Yu, W.H., Ren, J., Chen, W., Huang, L., Kharbanda, S., Loda, M., and Kufe, D. (2003c). Heregulin targets gamma-catenin to the nucleolus by a mechanism dependent on the DF3/MUC1 oncoprotein. Mol. Cancer Res. *1*, 765–775.

Ligtenberg, M.J., Kruijshaar, L., Buijs, F., van Meijer, M., Litvinov, S.V., and Hilkens, J. (1992). Cell-associated episialin is a complex containing two proteins derived from a common precursor. J. Biol. Chem. *267*, 6171–6177.

Lin, S.Y., Makino, K., Xia, W., Matin, A., Wen, Y., Kwong, K.Y., Bourguignon, L., and Hung, M.C. (2001). Nuclear localization of EGF receptor and its potential new role as a transcription factor. Nat. Cell Biol. *3*, 802–808.

Loukas, A., Hintz, M., Linder, D., Mullin, N.P., Parkinson, J., Tetteh, K.K., and Maizels, R.M. (2000). A family of secreted mucins from the parasitic nematode Toxocara canis bears diverse mucin domains but shares similar flanking six-cysteine repeat motifs. J. Biol. Chem. *275*, 39600–39607.

Lukashev, M.E., and Werb, Z. (1998). ECM signalling: orchestrating cell behaviour and misbehaviour. Trends Cell Biol. *8*, 437–441.

Macao, B., Johansson, D.G., Hansson, G.C., and Hard, T. (2006). Autoproteolysis coupled to protein folding in the SEA domain of the membrane-bound MUC1 mucin. Nat. Struct. Mol. Biol. *13*, 71–76.

MacAulay, K., Doble, B.W., Patel, S., Hansotia, T., Sinclair, E.M., Drucker, D.J., Nagy, A., and Woodgett, J.R. (2007). Glycogen synthase kinase 3alpha-specific regulation of murine hepatic glycogen metabolism. Cell Metab. *6*, 329–337.

Matrisian, L.M., Wright, J., Newell, K., and Witty, J.P. (1994). Matrix-degrading metalloproteinases in tumor progression. Princess Takamatsu symp. *24*, 152–161.

Mitsiades, N., Yu, W.H., Poulaki, V., Tsokos, M., and Stamenkovic, I. (2001). Matrix metalloproteinase-7-mediated cleavage of Fas ligand protects tumor cells from chemotherapeutic drug cytotoxicity. Cancer Res. *61*, 577–581.

Muthuswamy, S.K., Li, D., Lelievre, S., Bissell, M.J., and Brugge, J.S. (2001). ErbB2, but not ErbB1, reinitiates proliferation and induces luminal repopulation in epithelial acini. Nat. Cell Biol. *3*, 785–792.

Nath, S., and Mukherjee, P. (2014). MUC1: a multifaceted oncoprotein with a key role in cancer progression. Trends Mol. Med. *20*, 332–342.

Ni, C.Y., Murphy, M.P., Golde, T.E., and Carpenter, G. (2001). Gamma -Secretase cleavage and nuclear localization of ErbB-4 receptor tyrosine kinase. Science *294*, 2179–2181.

Okorokov, A.L., and Milner, J. (1997). Proteolytic cleavage of p53: a model for the activation of p53 in response to DNA damage. Oncol Res. *9*, 267–273.

Orsolic, I., Jurada, D., Pullen, N., Oren, M., Eliopoulos, A.G., and Volarevic, S. (2015). The relationship between the nucleolus and cancer: current evidence and emerging paradigms. Semin. Cancer Biol. *37-38*, 36–50.

Pacheco, M.M., Mourao, M., Mantovani, E.B., Nishimoto, I.N., and Brentani, M.M. (1998). Expression of gelatinases A and B, stromelysin-3 and matrilysin genes in breast carcinomas: clinico-pathological correlations. Clin. Exp. Metastasis *16*, 577–585.

Parks, W.C., and Shapiro, S.D. (2001). Matrix metalloproteinases in lung biology. Respir. Res. *2*, 10–19.

Parry, S., Silverman, H.S., McDermott, K., Willis, A., Hollingsworth, M.A., and Harris, A. (2001). Identification of MUC1 proteolytic cleavage sites in vivo. Biochem. Biophys. Res. Commun. *283*, 715–720.

Pederson, T. (1998). Growth factors in the nucleolus? J. Cell Biol. *143*, 279–281.

Pelaseyed, T., Zach, M., Petersson, A.C., Svensson, F., Johansson, D.G., and Hansson, G.C. (2013). Unfolding dynamics of the mucin SEA domain probed by force spectroscopy suggest that it acts as a cell-protective device. FEBS J. *280*, 1491–1501.

Perl, A.K., Wilgenbus, P., Dahl, U., Semb, H., and Christofori, G. (1998). A causal role for E-cadherin in the transition from adenoma to carcinoma. Nature *392*, 190–193.

Perrin, L., Demakova, O., Fanti, L., Kallenbach, S., Saingery, S., Mal'ceva, N.I., Pimpinelli, S., Zhimulev, I., and Pradel, J. (1998). Dynamics of the sub-nuclear distribution of Modulo and the regulation of position-effect variegation by nucleolus in Drosophila. J. Cell. Sci. *111* (Pt 18), 2753–2761.

Petersen, O.H. (1992). Stimulus-secretion coupling: cytoplasmic calcium signals and the control of ion channels in exocrine acinar cells. J. Physiol. *448*, 1–51.

Polakis, P. (2000). Wnt signaling and cancer. Genes Dev. *14*, 1837–1851.

Powell, W.C., Fingleton, B., Wilson, C.L., Boothby, M., and Matrisian, L.M. (1999). The metalloproteinase matrilysin proteolytically generates active soluble Fas ligand and potentiates epithelial cell apoptosis. Curr. Biol. *9*, 1441–1447.

Ren, J., Li, Y., and Kufe, D. (2002). Protein kinase C delta regulates function of the DF3/MUC1 carcinoma antigen in beta-catenin signaling. J. Biol. Chem. *277*, 17616–17622.

Rudolph-Owen, L.A., Hulboy, D.L., Wilson, C.L., Mudgett, J., and Matrisian, L.M. (1997). Coordinate expression of matrix metalloproteinase family members in the uterus of normal, matrilysin-deficient, and stromelysin-1-deficient mice. Endocrinology *138*, 4902–4911.

Rudolph-Owen, L.A., Slayden, O.D., Matrisian, L.M., and Brenner, R.M. (1998). Matrix metalloproteinase expression in Macaca mulatta endometrium: evidence for zone-specific regulatory tissue gradients. Biol. Reprod. *59*, 1349–1359.

Ruggero, D., and Pandolfi, P.P. (2003). Does the ribosome translate cancer? Nat. Rev. Cancer *3*, 179–192.

Saarialho-Kere, U.K., Vaalamo, M., Puolakkainen, P., Airola, K., Parks, W.C., and Karjalainen-Lindsberg, M.L. (1996). Enhanced expression of matrilysin, collagenase, and stromelysin-1 in gastrointestinal ulcers. Am. J. Pathol. *148*, 519–526.

Sahraei, M., Roy, L.D., Curry, J.M., Teresa, T.L., Nath, S., Besmer, D., Kidiyoor, A., Dalia, R., Gendler, S.J., and Mukherjee, P. (2012). MUC1 regulates PDGFA expression during pancreatic cancer progression. Oncogene *31*, 4935–4945.

Schroeder, J.A., Thompson, M.C., Gardner, M.M., and Gendler, S.J. (2001). Transgenic MUC1 interacts with epidermal growth factor receptor and correlates with mitogen-activated protein kinase activation in the mouse mammary gland. J. Biol. Chem. *276*, 13057–13064.

Seshachar, B.R. (1948). The nucleolus of the apodan Sertoli cell. Nature *161*, 558.

Slomnicki, L.P., Pietrzak, M., Vashishta, A., Jones, J., Lynch, N., Elliot, S., Poulos, E., Malicote, D., Morris, B.E., Hallgren, J., and Hetman, M. (2016). Requirement of neuronal ribosome synthesis for growth and maintenance of the dendritic tree. J. Biol. Chem. *291*, 5721–5739.

Sonnenblick, B.P. (1948). Synchronous mitoses in Drosophila, their intensely rapid rate, and the sudden appearance of the nucleolus. Genetics *33*, 125.

Soule, H.D., Maloney, T.M., Wolman, S.R., Peterson, W.D., Jr., Brenz, R., McGrath, C.M., Russo, J., Pauley, R.J., Jones, R.F., and Brooks, S.C. (1990). Isolation and characterization of a spontaneously immortalized human breast epithelial cell line, MCF-10. Cancer Res. *50*, 6075–6086.

Takada, H., and Kurisaki, A. (2015). Emerging roles of nucleolar and ribosomal proteins in cancer, development, and aging. Cell. Mol. Life Sci. *72*, 4015–4025.

Thathiah, A., Blobel, C.P., and Carson, D.D. (2003). Tumor necrosis factor-alpha converting enzyme/ADAM 17 mediates MUC1 shedding. J. Biol. Chem. *278*, 3386–3394.

Tin, A.S., Park, A.H., Sundar, S.N., and Firestone, G.L. (2014). Essential role of the cancer stem/progenitor cell marker nucleostemin for indole-3-carbinol anti-proliferative responsiveness in human breast cancer cells. BMC Biol. *12*, 72.

Vermeer, P.D., Einwalter, L.A., Moninger, T.O., Rokhlina, T., Kern, J.A., Zabner, J., and Welsh, M.J. (2003). Segregation of receptor and ligand regulates activation of epithelial growth factor receptor. Nature *422*, 322–326.

Vleminckx, K., Vakaet, L., Jr., Mareel, M., Fiers, W., and van Roy, F. (1991). Genetic manipulation of E-cadherin expression by epithelial tumor cells reveals an invasion suppressor role. Cell *66*, 107–119.

Wang, F., Zhou, S., Qi, D., Xiang, S.H., Wong, E.T., Wang, X., Fonkem, E., Hsieh, T.C., Yang, J., et al. (2019). Nucleolin is a functional binding protein for salinomycin in neuroblastoma stem cells. J. Am. Chem. Soc. *141* (8), 3613–3622.

Weaver, C. (1997). Angioarchitecture of the atrophic pancreas. Microsc. Res. Tech. *37*, 520–542.

Wei, X., Xu, H., and Kufe, D. (2005). Human MUC1 oncoprotein regulates p53-responsive gene

transcription in the genotoxic stress response. Cancer Cell *7*, 167–178.

Wilson, C.L., Heppner, K.J., Labosky, P.A., Hogan, B.L., and Matrisian, L.M. (1997). Intestinal tumorigenesis is suppressed in mice lacking the metalloproteinase matrilysin. Proc. Natl. Acad. Sci. U S A *94*, 1402–1407.

Wilson, C.L., Ouellette, A.J., Satchell, D.P., Ayabe, T., Lopez-Boado, Y.S., Stratman, J.L., Hultgren, S.J., Matrisian, L.M., and Parks, W.C. (1999). Regulation of intestinal alpha-defensin activation by the metalloproteinase matrilysin in innate host defense. Science *286*, 113–117.

Witty, J.P., McDonnell, S., Newell, K.J., Cannon, P., Navre, M., Tressler, R.J., and Matrisian, L.M. (1994). Modulation of matrilysin levels in colon carcinoma cell lines affects tumorigenicity in vivo. Cancer Res. *54*, 4805–4812.

Woessner, J.F., Jr. (1996). Regulation of matrilysin in the rat uterus. Biochem. Cell Biol. *74*, 777–784.

Woods, S.J., Hannan, K.M., Pearson, R.B., and Hannan, R.D. (2015). The nucleolus as a fundamental regulator of the p53 response and a new target for cancer therapy. Biochim. Biophys. Acta *1849*, 821–829.

Wreschner, D.H., McGuckin, M.A., Williams, S.J., Baruch, A., Yoeli, M., Ziv, R., Okun, L., Zaretsky, J., Smorodinsky, N., Keydar, I., et al. (2002). Generation of ligand-receptor alliances by "SEA" module-mediated cleavage of membrane-associated mucin proteins. Protein Sci. *11*, 698–706.

Yamamoto, M., Bharti, A., Li, Y., and Kufe, D. (1997). Interaction of the DF3/MUC1 breast carcinoma-associated antigen and beta-catenin in cell adhesion. J. Biol. Chem. *272*, 12492–12494.

Yamashita, N., Fushimi, A., Kui, L., Samur, M., Yamamoto, M., Zhang, Y., Zhang, N., Hong, D., Maeda, T., Kosaka, T., Wong, K.K., Oya, M., and Kufe, D. (2020). MUC1-C regulates lineage plasticity driving progression to neuroendocrine prostate cancer. Nat. Commun. *11* (338), 1–13.

Yang, A., Shi, G., Zhou, C., Lu, R., Li, H., Sun, L., and Jin, Y. (2011). Nucleolin maintains embryonic stem cell self-renewal by suppression of p53 protein-dependent pathway. The Journal Biological Chemistry *286*, 43370–43382.

Yin, L., Li, Y., Ren, J., Kuwahara, H., and Kufe, D. (2003). Human MUC1 carcinoma antigen regulates intracellular oxidant levels and the apoptotic response to oxidative stress. J. Biol. Chem. *278*, 35458–35464.

Yin, L., Tagde, A., Gali, R., Tai, Y.T., Hideshima, T., Anderson, K., Avigan, D., and Kufe, D. (2017). MUC1-C is a target in lenalidomide resistant multiple myeloma. Br. J. Haematol. *178*, 914–926.

Yu, W.H., Huang, P.T., Lou, K.L., Yu, S.S., and Lin, C. (2012). A smallest 6 kda metalloprotease, mini-matrilysin, in living world: a revolutionary conserved zinc-dependent proteolytic domain-helix-loop-helix catalytic zinc binding domain (ZBD). J. Biomed. Sci. *19*, 54.

Yu, W.H., and Woessner, J.F., Jr. (2000). Heparan sulfate proteoglycans as extracellular docking molecules for matrilysin (matrix metalloproteinase 7). J. Biol. Chem. *275*, 4183–4191.

Yu, W.H., and Woessner, J.F., Jr. (2001). Heparin-enhanced zymographic detection of matrilysin and collagenases. Anal. Biochem. *293*, 38–42.

Yu, W.H., Woessner, J.F., Jr., McNeish, J.D., and Stamenkovic, I. (2002). CD44 anchors the assembly of matrilysin/MMP-7 with heparin-binding epidermal growth factor precursor and ErbB4 and regulates female reproductive organ remodeling. Genes Dev. *16*, 307–323.

Zhou, W., and Carpenter, G. (2000). Heregulin-dependent trafficking and cleavage of ErbB-4. J. Biol. Chem. *275*, 34737–34743.

iScience, Volume *23*

Supplemental Information

Matrix Metalloprotease-7 Mediates Nucleolar Assembly and Intra-nucleolar Cleaving p53 in Gefitinib-Resistant Cancer Stem Cells

Wei-Hsuan Yu, Erxi Wu, Yongqing Li, Hsin-Han Hou, Shuan-su C. Yu, Po-Tsang Huang, Wen-Hung Kuo, Dan Qi, and Chong-Jen Yu

Transparent Methods

Cell cultures

Human ZR-75-1 breast carcinoma cells (ATCC, Manassas, VA) were cultured in a RPMI 1640 high-glucose medium containing 10% heat-inactivated fetal bovine serum (HI-FBS), 100 units/mL penicillin, 100 µg/mL streptomycin and 2 mM L-glutamine. Human MCF-10A breast epithelial cells were grown in a DMEM-F12 medium containing 5% heat-inactivated horse serum, 20 ng/mL EGF, 500 ng/mL hydrocortisone, 100 ng/mL cholera toxin and 10 µg/mL insulin. Human HCT116 carcinoma cells were cultured in Dulbecco's Modified Eagle's Medium containing 10% HI-FBS and antibiotics. Cells grown to 70% confluency were maintained in a medium containing 0.1% HI-FBS for 18 h and then stimulated with 20 ng/mL HRG (Calbiochem-Novabiochem, San Diego, CA) or 1 µM PMA/TPA (Sigma, St. Louis, MO) at 37 °C. Cells were also grown to 70% confluency, fixed with 100% methanol, washed with PBS containing Mg^{2+}/Ca^{2+} and treated with 100 ng/mL MMP-7 (Yu et al., 2002), 200 ng/mL MMP-2 (Troeberg et al., 2002), 200 ng/mL MMP-9 (Itoh and Nagase, 1995), and 500 ng/mL TIMP-1/-2 (Itoh and Nagase, 1995), 500 ng/mL TIMP-3 or N-TIMP-3 (Yu and Woessner, 2001; Yu et al., 2002) for 4 h at 37 °C.

Soft agar assay

In a six-well plate, cells were seeded at 2500 cells per well in 0.3% Agarose DMEM + 10% FCS in the top gel layer and 0.7% agarose gel DMEM in the bottom gel layer. Plates were incubated at 37 °C in a humidified incubator for 20-30 days. Cells were fed 1-2 times per week with cell culture media. Plates were stained with 0.5 ml of 0.005%

Crystal Violet for more than 1 hour for quantitation. Colonies were picked up by using a dissecting microscope.

Immunoprecipitation and immunoblotting

Cell surface molecules were co-immunoprecipitated following the pre-incubation of cells in blocking solution (4% goat serum, 50 μM ZnCl2, and the protease inhibitors ZPCK, PMSF, AEBSF, leupeptin and phosphoramidonin PBS). Cell or nuclear extracts were then incubated with anti-MUC-1 N-ter (Kufe et al., 1984), anti-MMP-7 (Yu et al., 2002) , anti-nucleolin, and anti-MUC-1-CD overnight at 4 °C in blocking solution, washed extensively with 50 μM ZnCl2/PBS and lysed with 1.25% Triton X-100, 50 mM Tris-HCl, pH 7.5, 0.15 M NaCl, 100 μM $ZnCl_2$, 5 mM $MgCl_2$, 50 μM $ZnCl_2$, 50 μM each of ZPCK, TPCK, and TLCK, 500 μM 4-(2-aminoethyl)-benzenesulfonyl chloride (Calbiochem-Novabiochem, San Diego, CA) and 1 μg/mL each of aprotinin, leupeptin and pepstatin (Sigma). The lysates were cleared by centrifugation at 16,000 x g for 15 min at 4 °C. The cell surface complexes were immunoprecipitated by incubation with Kappa-lock beads (Zymed Laboratories, San Francisco, CA) for 45 min at room temperature. After centrifugation, the precipitates were washed with 0.25% Triton X-100, 50 mM Tris-HCl, pH 7.5, 0.15 M NaCl, 10 mM $CaCl_2$, 5 mM $MgCl_2$ and 50 μM $ZnCl_2$. The samples were loaded in a non-reducing SDS sample buffer, subjected to electrophoresis and transferred to a 0.45 μm pore-size nitrocellulose membrane. Immunoblotting was performed with anti-MMP-7(RM7C), anti-nucleolin, anti-CD44v3 mAb (R&D Systems), and anti-MUC-1 CD (Li et al., 2003a).

In vitro cleavage of MUC-1

Anti-MUC-1 N-ter immunoprecipitates were washed in PBS containing 25 μM EDTA to deplete endogenous MMP-7, followed by washing with 0.25% Triton X-100, 50 μM Tris-HCl, pH 7.5, 0.15 M NaCl, 10 mM CaCl2 and 5 mM MgCl2. E. coli-derived purified active human MMP-7 (approximately 50 ng/mL) (Yu and Woessner, 2000) was added to the complexes in the absence and presence of 100 nM SC44463 (Abramson and Woessner, 1994), which were incubated overnight at 37 °C. As a control, the complexes were incubated with active MMP-9 prepared from mammalian cells (Abramson and Woessner, 1994). The reaction products were analyzed by immunoblotting with anti-MUC-1 C-ter.

A MUC-1 extracellular domain (ECD)-Fc fusion protein was generated by amplifying DNA sequences encoding the NUC1 (ECD) with the following primers: sense, 5'-CTAGCTAGCATGACACCGGGCACCCAGTC; and anti-sense, 5'-CGCGGATCCCCCAGCCCCAGACTGG. The PCR product was digested with Nhe1 and BamH1 and then inserted into the peak 13CD51neg1 vector (kindly provided by Dr. Brian Seed). The MUC-1 (ECD)-Fc plasmid was transiently transfected into 293 cells. The supernatant was harvested, and the MUC-1 (ECD)-Fc fusion protein was affinity-purified on a protein A-Sepharose column.

In the in-situ recombinant active MMP-7 digestion

ZR-75-1 cells were grown on a cover slip to 70~80% confluency, then metabolically stopped with 50 mM sodium azide (NaN3) for 10 minutes, after which cells were shortly fixed with 4% paraformaldehyde for 3 minutes, followed by a wash with 500 ml PBS 3X at RT for 20 minutes. Next, the fixed coverslips were incubated with 300 ng purified E.Coli derived active recombinant MMP-7 in the presence or absence of synthetic inhibitor SC44463 in the incubation buffer at 37 ^{o}C for 6 hours. Then the immunofluorescent

staining was performed with the anti-N-terminal MUC-1(anti-MUC-1 N-ter) antibody followed by the immunofluorescence staining protocol.

Confocal microscopy

Cells were pre-fixed with 3.7% formaldehyde in PBS containing Mg^{2+}/Ca^{2+}. Paraffin-embedded tissues were de-waxed by treating the sections with xylene for 5 min x 3, followed by washing with 100% ethanol for 5 min x 3 and 3% H_2O_2/methanol for 10 min. The cells and tissue sections were blocked with heat-inactivated control serum (same species as the secondary antibody) for 18 h at 4 °C. The samples were 1) incubated with anti-MUC-1 N-ter, anti-MUC-1 C-ter, anti-MMP-7, anti-γ-catenin (Zymed Laboratories) or anti-nucleolin (Hasegawa et al., 2016) for 18 h at 4 °C; 2) washed with PBS containing Mg^{2+}/Ca^{2+}, 3) incubated with secondary fluorescein- or Texas Red-conjugated polyclonal anti-IgG antibodies (Jackson Immunoresearch Laboratories, West Grove, PA) for 45 min at room temperature; 4) washed in PBS containing Mg^{2+}/Ca^{2+}; and 5) analyzed by confocal microscopy (inverted Zeiss LSM 510). Excitation was conducted at 488 nm and 543 nm, and emission was conducted at 505 nm and 585 nm for fluorescein isothiocyanate and Texas Red, respectively. Nuclear staining with TOTO-3 (Molecular Probes, Eugene, OR) was detected at an excitation of 642 nm and emission of 660 nm. Images were captured at 0.6 nm increments along the z-axis and converted to composites using the LSM software.

Heparin-enhanced carboxymethylated (CM)-transferrin substrate zymography

Protein samples containing 0.5 μg/mL heparin sulfate were subjected to CM-transferrin substrate zymography as previously described (Yu and Woessner, 2001). The gels were washed with 1) 2.5% Triton X-100, 50 mM Tris-HCl, pH 7.5, at 4°C to remove SDS; 2) the same buffer supplemented with 5 mM $CaCl_2$; 3) incubation buffer (50 mM Tris-HCl, pH 7.5, 5 mM $CaCl_2$); and 4) incubation buffer containing ZPCK, TPCK, TLCK and 4-(2-aminoethyl)-benzenesulfonyl chloride for 18 h at 37°C with gentle shaking. The gels were stained with 0.1% Coomassie brilliant blue in 40% methanol and 10% acetic acid and destained with 7% acetic acid.

MUC-1 siRNA

A pair of DNA oligos that target MUC-1, 5'-TCG AGG CCA GGA TCT GTG GTG GTA CGA GTA CTG GTA CCA CCA CAG ATC CTG GCC TTT TT-3' and 5'-CTA GAA AAA GGC CAG GAT CTG TGG TGG TAC CAG TAC TCG TAC CAC CAC AGA TCC TGG CC-3', were ligated into the pSuppressor Retro vector (Imgenex, San Diego, CA). Following sequence verification, the empty or MUC-1 siRNA retrovirus vector and the pCL-Ampho packaging vector were cotransfected into 293 cells using the Gene-Jammer transfection reagent (Clontech). Stable transfectants were selected in the presence of G418. Conditioned medium containing the retroviruses was used for infection. Cells infected with the retroviruses were selected in 300 μg/mL G418.

Growth of mammary acinar structures

MCF-10A cells (~5000/well) were grown in 6% Matrigel as described (Muthuswamy et al., 2001). *E. coli*-derived N-TIMP-3 (50 ng/ml) (Yu and Woessner, 2000) or 100 nM SC44463

was added to the medium on day 3. Cells were infected with control or MUC-1 siRNA retroviruses on day 2. The stably transfected nucleolin-YFP/or GFP cells pool were maintained, and the nucleolar activities were analyzed in situ by confocal microscopy.

Establish the nucleolar activities in situ window-Nucleolin-YFP/or GFP transfected EGFR$^{L858R/T790M}$ CL1-0 small lung carcinoma cells

The mammalian expression nucleolin-YFP vector was constructed and transfected into EGFR$^{L858R/T790M}$ CL1-0 small lung carcinoma cells. The stable transfected nucleolin-YFP/or GFP cells pool was maintained. The *in situ* nucleolar activities were analyzed by confocal microscopy.

Homology modeling and docking MUC-1 SEA domain to mature MMP-7

The bell laboratory-layered space-time algorithm was used to search the protein data bank (PDB) for protein segments (SEA domain: S59-V162) for sequences that were similar to those of MUC-1 (NCBI accession number: NP_002447.4). Knowledge regarding human MUC-1 has been advanced by X-ray crystal structures (MUC-1 PDB code: 2ACM) (Macao et al., 2006). The Protein Data Bank (PDB) was then searched for protein segments with sequences (Y95-Y258) similar to those of MMP-7 (NCBI accession number: NP_002414.1) and structures that could serve as viable structural templates. Knowledge regarding mature MUC-1 has recently been advanced by X-ray crystal structures (MMP-7 PDB code: 2Y6D) (Edman et al., 2011).

Model building, loop generating and residue side chain simulation

Homology modeling was performed following previously described procedures (Chen et al., 2012; Huang et al., 2002; Pierce et al., 2014). Briefly, the residues of the un-cleaved/cleaved MUC-1 SEA domain and mature MMP-7, which were chosen according to the results of the GCG paired sequence alignment, were superimposed onto the structural coordinates of the Cα atoms of the corresponding SCRs from the template structures (PDB ID: 2ACM, 2Y6D). This procedure generated the secondary structure and relative positions of the definite structural elements in the chosen residues of the models. Junctions between secondary structural elements were determined according to the 10 choices provided by the software (Insight II model, Accelrys Inc., San Diego, CA). We chose the loop with the lowest energy and the root mean square deviation, in combination with slight manual adjustments, when short contacts were observed. After all operations were accomplished, the overall energy minimization was performed again to obtain the final model. Hydrophobic/hydrophilic interactions between the residue side chains were observed in the model to provide the required structural functional interpretation. All calculations and structure manipulations were performed using the Discover/Insight II molecular simulation and modeling program (Accelrys Inc., San Diego, CA; release 950) using the Silicon Graphics Octane/SSE and O2/R12000 workstations and an O-300 server.

Molecular Docking

We used the rigid-body molecular docking program ZDOCK 3.0.2 to survey possible initial binding modes of mature MMP-7 and un-cleaved/cleaved MUC-1. Each docking calculation generated 500 structures, as described by Rong's group (Chen et al., 2012;

Huang et al., 2002; Pierce et al., 2014). The structures containing the MUC-1 SEA domain were located near the active site of mature MMP-7 because MMP-7 binds to MUC-1 C-ter. Subsequently, cluster analysis with a MUC-1 SEA domain backbone RMSD cutoff of 20 Å was performed on the remaining structures to identify distinct binding modes for mature MMP-7.

CSC proliferation in BALBc/nu mice xenografts

This study conformed to the Guide for the Care and Use of Laboratory Animals published by the US National Institutes of Health (NIH Publication No. 85-23, revised 1996). All animal experiments were approved by the Institutional Animal Care and Use Committee (IACUC) of the Laboratory Animal Center, College of Medicine and Public Health, National Taiwan University. Six-week-old male BALBc/nu mice were purchased from the National Laboratory Animal Center, National Applied Research Laboratories. Six-week-old BALBc/nu mice were housed in groups of four mice per cage in an isolator. CSCs xenografts were grown by subcutaneously inoculating the dorsal region of each animal with 2 x 10^6 cells in 0.2 ml Hank's balanced salt solution for 28 days (Hidayat et al., 2019). 60 mg/kg/day gefitinib or 5 mg/kg/day of salinomycin were delivered by subcutaneously implanted osmotic pump for further 28 days.

Supplemental References

Abramson, S. R., and Woessner, J. F., Jr. (1994). Characterization of rat matrilysin and its cDNA. Annals of the New York Academy of Sciences *732*, 362-364.

Chen, R., Robinson, A., and Chung, S. H. (2012). Binding of hanatoxin to the voltage sensor of Kv2.1. Toxins (Basel) *4*, 1552-1564.

Edman, K., Furber, M., Hemsley, P., Johansson, C., Pairaudeau, G., Petersen, J., Stocks, M., Tervo, A., Ward, A., Wells, E., and Wissler, L. (2011). The discovery of MMP7 inhibitors exploiting a novel selectivity trigger. ChemMedChem *6*, 769-773.
Hasegawa, M., Takahashi, H., Rajabi, H., Alam, M., Suzuki, Y., Yin, L., Tagde, A., Maeda, T., Hiraki, M., Sukhatme, V. P., and Kufe, D. (2016). Functional interactions of the cystine/glutamate antiporter, CD44v and MUC1-C oncoprotein in triple-negative breast cancer cells. Oncotarget *7*, 11756-11769.
Hidayat, M., Mitsuishi, Y., Takahashi, F., Tajima, K., Yae, T., Miyahara, K., Hayakawa, D., Winardi, W., Ihara, H., Koinuma, Y., *et al*. (2019). Role of FBXW7 in the quiescence of gefitinib-resistant lung cancer stem cells in EGFR-mutant non-small cell lung cancer. Bosn J Basic Med Sci.
Huang, P. T., Chen, T. Y., Tseng, L. J., Lou, K. L., Liou, H. H., Lin, T. B., Spatz, H. C., and Shiau, Y. Y. (2002). Structural influence of hanatoxin binding on the carboxyl terminus of S3 segment in voltage-gated K(+)-channel Kv2.1. Receptors Channels *8*, 79-85.
Itoh, Y., and Nagase, H. (1995). Preferential inactivation of tissue inhibitor of metalloproteinases-1 that is bound to the precursor of matrix metalloproteinase 9 (progelatinase B) by human neutrophil elastase. The Journal of biological chemistry *270*, 16518-16521.
Kufe, D., Inghirami, G., Abe, M., Hayes, D., Justi-Wheeler, H., and Schlom, J. (1984). Differential reactivity of a novel monoclonal antibody (DF3) with human malignant versus benign breast tumors. Hybridoma *3*, 223-232.
Li, Y., Yu, W. H., Ren, J., Chen, W., Huang, L., Kharbanda, S., Loda, M., and Kufe, D. (2003c). Heregulin targets gamma-catenin to the nucleolus by a mechanism dependent on the DF3/MUC1 oncoprotein. Molecular cancer research : MCR *1*, 765-775.
Macao, B., Johansson, D. G., Hansson, G. C., and Hard, T. (2006). Autoproteolysis coupled to protein folding in the SEA domain of the membrane-bound MUC1 mucin. Nat Struct Mol Biol *13*, 71-76.
Muthuswamy, S. K., Li, D., Lelievre, S., Bissell, M. J., and Brugge, J. S. (2001). ErbB2, but not ErbB1, reinitiates proliferation and induces luminal repopulation in epithelial acini. Nature cell biology *3*, 785-792.
Pierce, B. G., Wiehe, K., Hwang, H., Kim, B. H., Vreven, T., and Weng, Z. (2014). ZDOCK server: interactive docking prediction of protein-protein complexes and symmetric multimers. Bioinformatics *30*, 1771-1773.
Troeberg, L., Tanaka, M., Wait, R., Shi, Y. E., Brew, K., and Nagase, H. (2002). E. coli expression of TIMP-4 and comparative kinetic studies with TIMP-1 and TIMP-2: insights into the interactions of TIMPs and matrix metalloproteinase 2 (gelatinase A). Biochemistry *41*, 15025-15035.
Yu, W. H., and Woessner, J. F., Jr. (2000). Heparan sulfate proteoglycans as extracellular docking molecules for matrilysin (matrix metalloproteinase 7). The Journal of biological chemistry *275*, 4183-4191.
Yu, W. H., and Woessner, J. F., Jr. (2001). Heparin-enhanced zymographic detection of matrilysin and collagenases. Analytical biochemistry *293*, 38-42.
Yu, W. H., Woessner, J. F., Jr., McNeish, J. D., and Stamenkovic, I. (2002). CD44 anchors the assembly of matrilysin/MMP-7 with heparin-binding epidermal growth factor precursor and ErbB4 and regulates female reproductive organ remodeling. Genes & development *16*, 307-323.